NATIONAL ADVISORY COMMITTEE
FOR AERONAUTICS

TECHNICAL NOTE 4048

MOTION OF A BALLISTIC MISSILE ANGULARLY MISALIGNED WITH
THE FLIGHT PATH UPON ENTERING THE ATMOSPHERE AND ITS
EFFECT UPON AERODYNAMIC HEATING, AERODYNAMIC
LOADS, AND MISS DISTANCE

By H. Julian Allen

Ames Aeronautical Laboratory
Moffett Field, Calif.

P

TECHNICAL NOTE 4048

MOTION OF A BALLISTIC MISSILE ANGULARLY MISALIGNED WITH THE FLIGHT PATH UPON ENTERING THE ATMOSPHERE AND ITS EFFECT UPON AERODYNAMIC HEATING, AERODYNAMIC LOADS, AND MISS DISTANCE[1]

By H. Julian Allen

SUMMARY

An analysis is given of the oscillating motion of a ballistic missile which upon entering the atmosphere is angularly misaligned with respect to the flight path. The history of the motion for some example missiles is discussed from the point of view of the effect of the motion on the aerodynamic heating and loading. The miss distance at the target due to misalignment and to small accidental trim angles is treated. The stability problem is also discussed for the case where the missile is tumbling prior to atmospheric entry.

INTRODUCTION

It is characteristic of long-range rockets that, because of the low efficiency of the propulsion system, the weight at take-off is large compared to the final weight after fuel is expended. Typically, a saving of 1 pound in final weight can save of the order of 20 pounds of initial weight and, as a result, strict attention must be given in the design of rockets to keep design safety factors to a minimum. Thus the magnitude of the factors which principally influence the final weight must be known with as great accuracy as possible.

Two such factors are the aerodynamic load experienced by the vehicle as it descends through the atmosphere, which affects required structural weight, and the aerodynamic heating experienced in the descent, which affects required coolant weight. Problems relating to the loading and heating of missiles during atmospheric entry have, of course, been given considerable attention, both from a general point of view (e.g., ref. 1) and in detail for specific designs. In the usual treatment of the problem, however, the rather idealized case has been treated wherein the vehicle enters the atmosphere unyawed or unpitched with respect to the flight path and without angular velocity. If the vehicle enters the atmosphere in a yawed or pitched attitude, it will, during its oscillatory approach to the earth, be subjected to lateral forces in addition to the longitudinal forces due to deceleration. Moreover, the distribution of

---

[1]Supersedes NACA RM A56F15 by H. Julian Allen, 1956.

66 p.

aerodynamic heating over the surface for the oscillating vehicle will differ from that for the vehicle if aligned with the flight path. Thus a question arises as to what extent the structural weight and the weight of coolant might-be altered by the fact that the rocket upon entering the atmosphere is angularly misaligned and has angular velocity.

The analysis of reference 2 provides an excellent basis for such a study. However, the results of that analysis are in a form which is not convenient for demonstrating the relative importance of the several factors which are of principal interest to the loading and heating problems. It is the purpose of this paper to re-examine the motion analysis of reference 2 using some simplifications which were employed in reference 1 in order to indicate more clearly the salient features of the motion problem and its effect, in turn, on loading and heating.[2]

BASIC ASSUMPTIONS

In the analysis to follow it will be assumed that the missile warhead which enters the atmosphere is rotationally symmetric so the misalignment angle may be considered as yaw or pitch or any vector combination thereof, and that the fineness ratio is sufficiently low and the Mach number is sufficiently high that the pressure distribution is independent of Mach number for the Mach number range of importance (see ref. 4). Thus, the rates of change of the respective aerodynamic force and moment coefficients with α, $\dot{\alpha}$, and q are considered to be constants. The basic assumption of the analysis of reference 2 is retained in the analysis to follow; namely, that the angular oscillations are small so that the sine of the angle of oscillation is the angle of oscillation in radians and the cosine is unity, and the drag coefficient is sensibly the same as it would be for the nonoscillating missile. In addition, the assumptions employed in reference 1 are also employed herein; namely, that the acceleration of gravity is constant with altitude, the flight path through the atmosphere is essentially a straight line, and the variation of air density is the exponential function

$$\rho = \rho_0 e^{-\beta y} \qquad \qquad (1)$$

wherein ρ_0 and β are constants and y is the altitude measured from sea level.

A complete list of symbols is given in Appendix A.

[2]It should be noted that an analysis has been made in reference 3 which, although principally aimed at study of other features of the stability problem, employs a basic approach similar to that of the present report.

ANALYSIS

If the angular displacements are small, then the differential equation of angular motion with time as the independent variable may be written

$$\frac{d^2\alpha}{dt^2} + f_1(t)\,\frac{d\alpha}{dt} + f_2(t)\alpha = 0 \tag{2}$$
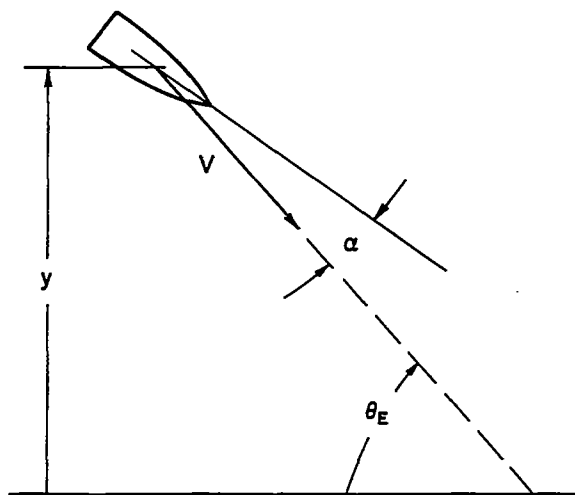
wherein the time-dependent coefficients are given by[3]

$$f_1(t) = \frac{C_{L_\alpha}\rho VA}{2m} - \frac{(C_{m_q} + C_{m_{\dot\alpha}})\rho VAl^2}{2I} \tag{3a}$$

$$f_2(t) = \frac{d}{dt}\left(\frac{C_{L_\alpha}\rho VA}{2m}\right) - \frac{C_{m_q}C_{L_\alpha}\rho^2 V^2 A^2 l^2}{4Im} - \frac{C_{m_\alpha}\rho V^2 Al}{2I} \tag{3b}$$

where the angle of attack is as indicated in the sketch.

[3]This formulation is equivalent to equations (12) and (13) in reference 2 except that in reference 2 the value of $C_{m_{\dot\alpha}}$ has been tacitly assumed to be zero, which is a justifiable assumption at high Mach numbers. The quantity $C_{m_{\dot\alpha}}$ is retained in equation (3a) to be consistent with NACA standard nomenclature (e.g., see ref. 5).

It is convenient, now, to rewrite equation (2) with altitude, y, rather than time, t, as the independent variable. To this end, it is noted that for the straight flight path assumed ($\theta = \theta_E = $ constant)

$$\frac{dy}{dt} = -V \sin \theta_E \tag{4a}$$

$$\frac{d^2y}{dt^2} = -\frac{dV}{dy} \frac{dy}{dt} \sin \theta_E = V \frac{dV}{dy} \sin^2\theta_E \tag{4b}$$

Thus

$$\frac{d\alpha}{dt} = \frac{d\alpha}{dy} \frac{dy}{dt} = -V \sin \theta_E \frac{d\alpha}{dy} \tag{5a}$$

$$\frac{d^2\alpha}{dt^2} = \frac{d^2\alpha}{dy^2} \left(\frac{dy}{dt}\right)^2 + \frac{d\alpha}{dy} \frac{d^2y}{dt^2} = V^2\sin^2\theta_E \frac{d^2\alpha}{dy^2} + V \frac{dV}{dy} \sin^2\theta_E \frac{d\alpha}{dy} \tag{5b}$$

so that equation (2) becomes

$$\frac{d^2\alpha}{dy^2} + f_3(y) \frac{d\alpha}{dy} + f_4(y)\alpha = 0 \tag{6}$$

wherein the altitude-dependent coefficients are

$$f_3(y) = \frac{dV/dy}{V} - \frac{C_{L_\alpha}\rho A}{2m \sin \theta_E} + \frac{(C_{m_q} + C_{m_{\dot\alpha}})\rho A l^2}{2I \sin \theta_E} \ . \tag{7a}$$

$$f_4(y) = -\frac{C_{L_\alpha}A(d\rho/dy)}{2m \sin \theta_E} - \frac{C_{L_\alpha}A\rho(dV/dy)}{2mV \sin \theta_E} - \frac{C_{m_q}C_{L_\alpha}\rho^2 A^2 l^2}{4Im \sin^2\theta_E} - \frac{C_{m_\alpha}\rho A l}{2I \sin^2\theta_E} \qquad (7b)$$

It is shown in reference 1 that by use of the same basic assumptions as have been made in this report, the velocity may be expressed as

$$V = V_E e^{-\frac{k_0}{2}} e^{-\beta y} \qquad (8a)$$

where

$$k_0 = \frac{C_D \rho_0 A}{\beta m \sin \theta_E} . \qquad (8b)$$

Hence

$$\frac{dV/dy}{V} = \frac{\beta k_0}{2} e^{-\beta y} \qquad 8(c)$$

and from equation (1)

$$\frac{d\rho}{dy} = -\beta \rho_0 e^{-\beta y} \qquad (8d)$$

Thus equations (7a) and (7b) become, upon setting the square of the radius of gyration as $\sigma^2 = I/m$,

$$f_3(y) = \frac{\rho_0 A}{2m \sin \theta_E}\left[C_D - C_{L_\alpha} + \frac{(C_{m_q} + C_{m_{\dot\alpha}})l^2}{\sigma^2}\right]e^{-\beta y} \qquad (9a)$$

$$f_4(y) = \frac{\rho_0 A}{2m \sin^2\theta_E}\left[-\frac{C_{m_\alpha}l}{\sigma^2} + C_{L_\alpha}\beta \sin \theta_E\right]e^{-\beta y} + \frac{\rho_0^2 A^2}{4m^2 \sin^2\theta_E}\left[-C_{L_\alpha}C_D - \frac{C_{m_q}C_{L_\alpha}l^2}{\sigma^2}\right]e^{-2\beta y} \qquad (9b)$$

If we set

$$Y = \beta y \tag{10a}$$

then equation (6) may be written

$$\frac{d^2\alpha}{dY^2} + 2k_1 e^{-Y} \frac{d\alpha}{dY} + \left(k_2 e^{-Y} + k_3 e^{-2Y}\right)\alpha = 0 \tag{10b}$$

wherein the constants are

$$\left.\begin{aligned}
k_1 &= \frac{\rho_o A}{4\beta m \sin \theta_E}\left[C_D - C_{L_\alpha} + (C_{m_q} + C_{m_{\dot\alpha}})\left(\frac{l}{\sigma}\right)^2\right] \\
k_2 &= \frac{\rho_o A}{2\beta^2 m \sin^2\theta_E}\left(-\frac{C_{m_\alpha} l}{\sigma^2} + C_{L_\alpha}\beta \sin \theta_E\right) \\
k_3 &= \frac{\rho_o{}^2 A^2}{4\beta^2 m^2 \sin^2\theta_E}\left[-C_{L_\alpha} C_D - C_{m_q} C_{L_\alpha}\left(\frac{l}{\sigma}\right)^2\right]
\end{aligned}\right\} \tag{10c}$$

In order to find a solution for the differential equation (10b) let

$$\alpha = \eta e^{k_1 e^{-Y}} \tag{11}$$

so that

$$\frac{d\alpha}{dY} = e^{k_1 e^{-Y}} \frac{d\eta}{dY} - k_1 e^{-Y} e^{k_1 e^{-Y}} \eta$$

and

$$\frac{d^2\alpha}{dY^2} = e^{k_1 e^{-Y}} \frac{d^2\eta}{dY^2} - 2k_1 e^{-Y} e^{k_1 e^{-Y}} \frac{d\eta}{dY} + \left(k_1 e^{-Y} e^{k_1 e^{-Y}} + k_1{}^2 e^{-2Y} e^{k_1 e^{-Y}}\right)\eta$$

Substitution in equation (10b) then yields

$$\frac{d^2\eta}{dY^2} + \left[(k_2 + k_1)e^{-Y} + (k_3 - k_1{}^2)e^{-2Y}\right]\eta = 0 \qquad (12)$$

The rigorous solution of this equation is not necessary since the term

$$(k_3 - k_1{}^2)e^{-2Y} \quad {}^{10^{-8}}$$

is, for the type of missiles to be considered later, small compared to

$$(k_2 + k_1)e^{-Y} \quad {}^{10^{-5}}$$

particularly at the higher altitudes which are of principal concern. If the square term is omitted, the solution of equation (12) is known (see, e.g., ref. 6)

$$\eta = C_1 J_0\!\left(2\sqrt{k_2 + k_1}\ e^{-\frac{Y}{2}}\right) + C_2 Y_0\!\left(2\sqrt{k_2 + k_1}\ e^{-\frac{Y}{2}}\right) \qquad (13)$$

where C_1 and C_2 are constants of integration and, in accordance with Watson's notation (ref. 7), the functions J_0 and Y_0 are the zero order Bessel functions of the first and second kind, respectively.

Combining equations (10a), (11), and (13) gives finally

$$\alpha = e^{k_1 e^{-\beta y}}\left[C_1 J_0\!\left(2\sqrt{k_2 + k_1}\ e^{-\frac{\beta y}{2}}\right) + C_2 Y_0\!\left(2\sqrt{k_2 + k_1}\ e^{-\frac{\beta y}{2}}\right)\right] \qquad (14)$$

If it is specified that on entering the atmosphere $(y \rightarrow \infty)$ the missile is misaligned by the angle α_E but has no angular velocity, then

$$\left.\begin{array}{l} C_1 = \alpha_E \\[2mm] C_2 = 0 \end{array}\right\} \qquad (15a)$$

and equation (14) can be written

$$\frac{\alpha}{\alpha_E} = e^{k_1 e^{-\beta y}} J_0\left(2\sqrt{k_2 + k_1}\ e^{-\frac{\beta y}{2}}\right) \tag{15b}$$

In the cases of usual interest the quantity k_2 is very much larger than k_1, as will be shown later, so that one may use the approximation

$$\frac{\alpha}{\alpha_E} = e^{k_1 e^{-\beta y}} J_0\left(2\sqrt{k_2}\ e^{-\frac{\beta y}{2}}\right) \tag{15c}$$

For large values of the argument, the approximation

$$\frac{\alpha}{\alpha_E} = \frac{e^{k_1 e^{-\beta y}}\cos\left(\frac{\pi}{4} - 2\sqrt{k_2}\ e^{-\frac{\beta y}{2}}\right)}{\sqrt{\pi\sqrt{k_2}\ e^{-\frac{\beta y}{2}}}} \tag{15d}$$

can be used, and the maximum or envelope value is thus

$$\left(\frac{\alpha}{\alpha_E}\right)^* = \frac{e^{k_1 e^{-\beta y}}}{\sqrt{\pi\sqrt{k_2}\ e^{-\frac{\beta y}{2}}}} \tag{15e}$$

In Appendix B are derived expressions for the angular velocity and angular acceleration as well as their maximum values during any cycle of oscillation. The approximate maximum angular velocity per cycle is (see eq. (B5c))

$$\left[\frac{d(\alpha/\alpha_E)}{dt}\right]^* = \sqrt{\frac{\sqrt{k_2}}{\pi}}\ \beta V_E \sin\theta_E e^{-\frac{\beta y}{4}} e^{\left(k_1 - \frac{k_0}{2}\right)e^{-\beta y}} \tag{15f}$$

while the maximum angular acceleration per cycle is

$$\left[\frac{d^2(\alpha/\alpha_E)}{dt^2}\right]^* = \frac{k_2^{\frac{3}{4}}}{\sqrt{\pi}}\beta^2 V_E^2 \sin^2\theta_E e^{-\frac{3\beta y}{4}} e^{(k_1-k_0)e^{-\beta y}} \qquad (15g)$$

From equation (15d) it can be found that one cycle of oscillation takes place during the altitude change

$$-\frac{2\pi}{\beta\sqrt{k_2}\ e^{-\frac{\beta y}{2}}}$$

The frequency of oscillation is thus

$$\omega = \frac{\beta\sqrt{k_2}\ e^{-\frac{\beta y}{2}}\ V\sin\theta_E}{2\pi}$$

and using the velocity from equation (8a) one has

$$\omega = \frac{\beta V_E\sqrt{k_2}\sin\theta_E}{2\pi}\ e^{-\frac{k_0}{2}}e^{-\beta y}\ e^{-\frac{\beta y}{2}} \qquad (16)$$

The frequency is maximum at the altitude

$$y_1 = \frac{1}{\beta}\ln k_0 \qquad (17a)$$

which, as shown in reference 1, is the altitude at which the deceleration due to drag is maximum and the velocity is

$$V_1 = e^{-\frac{1}{2}}V_E \cong 0.61\ V_E \qquad (17b)$$

The maximum frequency is

$$\omega_{max} = \omega_1 = \sqrt{\frac{k_2}{k_0}}\left(\frac{\beta V_E e^{-\frac{1}{2}}\sin\theta_E}{2\pi}\right) \qquad (17c)$$

and the corresponding amplitude is from equation (15e)

$$\left(\frac{\alpha}{\alpha_E}\right)^*_1 = \frac{e^{\frac{k_1}{k_0}}}{\sqrt{\pi \sqrt{\frac{k_2}{k_0}}}}$$ (17d)

For later use it is of importance to note that in the analysis of reference 1 it is shown that for turbulent flow the altitude for which the average heat-transfer rate is a maximum is

$$y_2 = \frac{1}{\beta} \ln\left(\frac{3}{2} k_0\right)$$ (18a)

when

$$V_2 = e^{-\frac{1}{3}} V_E \cong 0.72 \ V_E$$ (18b)

The corresponding frequency is

$$\omega_2 = \sqrt{\frac{2k_2}{3k_0}} \left(\frac{\beta V_E e^{-\frac{1}{3}} \sin \theta_E}{2\pi}\right)$$ (18c)

and the corresponding amplitude is

$$\left(\frac{\alpha}{\alpha_E}\right)^*_2 = \frac{e^{\frac{2k_1}{3k_0}}}{\sqrt{\pi \sqrt{\frac{2k_2}{3k_0}}}}$$ (18d)

On the other hand, for laminar flow (which, it is expected, should be applicable at least for the stagnation point on the missile nose), the altitude for maximum heating rate is then

$$y_3 = \frac{1}{\beta} \ln(3k_0)$$

when

$$V_3 = e^{-\frac{1}{6}} V_E \cong 0.85 V_E \qquad (19b)$$

and

$$\omega_3 = \sqrt{\frac{k_2}{3k_0}} \left(\frac{\beta V_E e^{-\frac{1}{6}} \sin \theta_E}{2\pi} \right) \qquad (19c)$$

and

$$\left(\frac{\alpha}{\alpha_E} \right)_3^* = \frac{e^{\frac{k_1}{3k_0}}}{\sqrt{\pi \sqrt{\frac{k_2}{3k_0}}}} \qquad (19d)$$

From a loads point of view it is of value to note that from equation (15g) the altitude for which the maximum angular acceleration occurs is

$$y_4 = \frac{1}{\beta} \ln\left[\frac{4}{3} (k_0 - k_1) \right] \qquad (20a)$$

and that the maximum acceleration is

$$\left[\frac{d^2(\alpha/\alpha_E)}{dt^2} \right]_{max}^* = \left[\frac{d^2(\alpha/\alpha_E)}{dt^2} \right]_4^* = \frac{1}{\sqrt{\pi}} \left[\frac{3k_2}{4(k_0 - k_1)} \right]^{\frac{3}{4}} e^{-\frac{3}{4}} \beta^2 V_E^2 \sin^2\theta_E \qquad (20b)$$

Also the normal force experienced is

$$N = \frac{1}{2} C_{N_\alpha} \alpha V^2 \rho A \qquad (21a)$$

and substitution from equations (1), (8a), and (15e) gives, for the maximum normal force per cycle

$$N^* = \frac{C_{N_\alpha} \alpha_E \rho_0 V_E^2 A}{2\sqrt{\pi \sqrt{k_2}}} e^{-\frac{3}{4}} \beta y_e (k_1 - k_0) e^{-\beta y} \qquad (21b)$$

This force is a maximum at y_4 and has the value

$$N_{max}^* = N_4^* = \frac{C_{N_\alpha}\alpha_E\rho_o V_E^2 A}{2\sqrt{\pi}\sqrt{k_2}}\left\{\left[\frac{3}{4(k_o - k_1)}\right]^{\frac{3}{4}} e^{-\frac{3}{4}}\right\} \qquad (21c)$$

Finally, it is of interest to determine the order of magnitude of the drift due to α_E from the course the missile would have had if aligned with the flight path. If n is defined as the distance normal to the straight line trajectory (that the missile would have if α_E were zero), the lateral acceleration is

$$\frac{d^2n}{dt^2} = -V \sin \theta_E \frac{d}{dy}\left(\frac{dn}{dt}\right) = \frac{L}{m} = \frac{C_{L_\alpha}\alpha V^2 \rho A}{2m} \qquad (22)$$

Use of the relations of equations (1), (8a), and (15c) gives the lateral velocity at altitude y

$$\frac{dn}{dt} = -\frac{C_{L_\alpha}\alpha_E V_E \rho_o A}{2m \sin \theta_E} \int_\infty^y e^{\left(k_1 - \frac{k_o}{2}\right)e^{-\beta y_1}} e^{-\beta y_1} J_o\left(2\sqrt{k_2} e^{-\frac{\beta y_1}{2}}\right) dy_1 \qquad (23a)$$

With the substitution

$$\zeta_1 = 2\sqrt{k_2} e^{-\frac{\beta y_1}{2}}$$

then this may be written

$$\frac{dn}{dt} = \frac{C_{L_\alpha}\alpha_E V_E \rho_o A}{4k_2\beta m \sin \theta_E} \int_o^{2\sqrt{k_2} e^{-\frac{\beta y}{2}}} e^{\left(\frac{k_1 - \frac{k_o}{2}}{4k_2}\right)\zeta_1^2} \zeta_1 J_o(\zeta_1) d\zeta_1 \qquad (23b)$$

The lateral displacement at $y = 0$ is, by similar substitution,

$$n = \frac{c_{L_\alpha}\alpha_E \rho_0 A}{2k_2 \beta^2 m \, \sin^2\theta_E} \int_0^{2\sqrt{k_2}} \frac{e^{\left(\frac{k_0}{8k_2}\right)\zeta^2}}{\zeta} \int_0^\zeta e^{\left(\frac{k_1 - \frac{k_0}{2}}{4k_2}\right)\zeta_1^2} \zeta_1 J_0(\zeta_1) d\zeta_1 d\zeta \quad (23c)$$

Defining

$$F(k_0,k_1,k_2) = \frac{1}{k_2} \int_0^{2\sqrt{k_2}} \frac{e^{\left(\frac{k_0}{8k_2}\right)\zeta^2}}{\zeta} \int_0^\zeta e^{\left(\frac{k_1 - \frac{k_0}{2}}{4k_2}\right)\zeta_1^2} \zeta_1 J_0(\zeta_1) d\zeta_1 d\zeta \quad (24a)$$

then

$$n = \frac{c_{L_\alpha}\alpha_E \rho_0 A}{2\beta^2 m \, \sin^2\theta_E} F(k_0,k_1,k_2) \quad (24b)$$

The integration of equation (24a) may be performed in the special case for which $k_1 = k_0 = 0$, for then

$$F(0,0,k_2) = \frac{1}{k_2} \int_0^{2\sqrt{k_2}} \frac{d\zeta}{\zeta} \int_0^\zeta \zeta_1 J_0(\zeta_1) d\zeta_1$$

$$= \frac{1}{k_2} \int_0^{2\sqrt{k_2}} J_1(\zeta) d\zeta = \frac{1 - J_0(2\sqrt{k_2})}{k_2} \cong \frac{1}{k_2}$$

For values of k_0 and k_1 other than zero, an analytic solution of equation (24a) is not known. However, Dr. William Mersman has determined values of the function by numerical integration using an IBM 650 type digital computer. The computational procedure and results are given in Appendix C. Over the range of variables of interest in this paper, $0 \leq k_0 \leq 10$, $-80 \leq k_1 \leq 0$, $5 \times 10^4 \leq k_2 \leq 8 \times 10^5$, the integration indicates that

$$F(k_0,k_1,k_2) = 1/k_2$$

within 0.2 percent (see Appendix C, eq. (C20)).

If the angle α_E is considered as a yaw angle then the miss distance is the lateral or "deflection target error"

$$\left(\epsilon_{\alpha_E}\right)_z = \frac{C_{L_\alpha}\alpha_E \rho_o A}{2\beta^2 m \, \sin^2\theta_E} \, F(k_0, k_1, k_2) \tag{25a}$$

while if the angle α_E is considered as a pitch error, then the miss distance is the longitudinal or "range target error"

$$\left(\epsilon_{\alpha_E}\right)_x = \frac{C_{L_\alpha}\alpha_E \rho_o A}{2\beta^2 m \, \sin^3\theta_E} \, F(k_0, k_1, k_2) \tag{25b}$$

Thus, in the general case, the area of miss is elliptical with the major axis in the range direction (except when the missile descent is vertical when the miss area is circular).

It is useful, for comparison purposes, to find the miss distance which results from an accidental trim angle, α_T. The differential equation (22) becomes in this case

$$\frac{d^2 n}{dt^2} = -V \sin \theta_E \, \frac{d}{dy}\left(\frac{dn}{dt}\right) = \frac{C_{L_\alpha}\alpha_T V^2 \rho A}{2m} \tag{26a}$$

so that

$$\frac{dn}{dt} = -\frac{C_{L_\alpha}\alpha_T \rho_o V_E A}{2m \sin \theta_E} \int_\infty^y e^{-\frac{k_0}{2}} \, e^{-\beta y_1} \, e^{-\beta y_1} dy_1$$

or

$$\frac{dn}{dt} = \frac{C_{L_\alpha}\alpha_T \rho_o V_E A}{k_0 \beta m \sin \theta_E} \left(1 - e^{-\frac{k_0}{2}} e^{-\beta y}\right) \tag{26b}$$

and, in turn,

$$n = \frac{C_{L_\alpha}\alpha_T \rho_o A}{k_0 \beta m \sin^2\theta_E} \int_\infty^0 \left(1 - e^{\frac{k_0}{2}} e^{-\beta y}\right) dy$$

which can be shown to give

$$n = \frac{C_{L_\alpha}\alpha_T\rho_oA}{\beta^2 m \; \sin^2\theta_E} \; F_1(k_o) \tag{26c}$$

wherein

$$F_1(k_o) = \frac{1}{k_o}\left[\overline{Ei}\!\left(\frac{k_o}{2}\right) - ln\!\left(\frac{k_o}{2}\right) - 0.577216\right] \tag{26d}$$

and $\overline{Ei}(k_o/2)$ is the exponential integral for which tabulated values are given in reference 8. Values of $F_1(k_o)$ have been computed for practical values of k_o and are presented in table I.

If the trim angle is a yaw angle then the miss distance is the deflection target error

$$\left(\epsilon_{\alpha_T}\right)_z = \frac{C_{L_\alpha}\alpha_T\rho_oA}{\beta^2 m \; \sin^2\theta_E} \; F_1(k_o) \tag{27a}$$

while if the trim angle is a pitch angle then the miss distance is the range target error

$$\left(\epsilon_{\alpha_T}\right)_x = \frac{C_{L_\alpha}\alpha_T\rho_oA}{\beta^2 m \; \sin^3\theta_E} \; F_1(k_o) \tag{27b}$$

DISCUSSION

Conical Warheads

It is the purpose in the discussion to follow to examine the angular motion of typical ballistic missiles in the atmosphere to ascertain the importance of this motion to the problems of aerodynamic loading and heating and miss distance. Conical shapes have been chosen for this study because the calculated stability derivatives are available.

Tobak and Wehrend (ref. 9) have calculated the stability derivatives for cones of half-angle, δ. Although they give results which are applicable

from low supersonic speeds (exceeding the Mach number for shock detachment) to hypersonic speeds, the concern of this paper will be only with the hypersonic or Newtonian solutions. For arbitrary distance from the cone apex to the center of gravity, l_{cg}, reference 9 gives the pertinent derivatives, using the symbols of this report, as

$$
\left.
\begin{aligned}
C_{N_\alpha} &= 2\cos^2\delta \\[6pt]
C_X &= C_D = 2\sin^2\delta \\[6pt]
C_{L_\alpha} &= C_{N_\alpha} - C_D = 2(\cos^2\delta - \sin^2\delta) \\[6pt]
C_{m_q} &= -(1 + \tan^2\delta) + \frac{8}{3}\left(\frac{l_{cg}}{l}\right) - 2\cos^2\delta\left(\frac{l_{cg}}{l}\right)^2 \\[6pt]
C_{m_{\dot{\alpha}}} &= 0 \\[6pt]
C_{m_\alpha} &= -\frac{4}{3} + 2\cos^2\delta\left(\frac{l_{cg}}{l}\right)
\end{aligned}
\right\}
\tag{28a}
$$

In addition it should be noted that for cones the center of volume is at $3l/4$ and the square of the ratio of cone length to radius of gyration for arbitrary center-of-gravity position is (considering the body to be uniformly solid)

$$
\left(\frac{l}{\sigma}\right)^2 = \frac{80}{12\tan^2\delta + 3 + 80\left(\frac{l_{cg}}{l} - \frac{3}{4}\right)^2}
\tag{28b}
$$

Validity of the Analysis

Before examining the stability, loading, heating, and miss-distance problems it is necessary to determine whether the previous analysis is valid for the conical shapes to be considered. It was noted that the solution given by equation (15b) applies only in those cases for which in the differential equation (12) the term

$$(k_3 - k_1{}^2)e^{-2Y} \qquad\qquad (29a)$$

can be neglected in comparison with

$$(k_2 - k_1)e^{-Y} \qquad\qquad (29b)$$

In Appendix D it is shown that the values of the factor (29a) are, for practical cases, always very small compared to the values of the factor (29b) and, in addition, that k_2 is, for practical cases, always much larger than k_1 so that the solution of equation (15c) is valid.

Stability

In the equation (15c) it is clear that the missile is statically stable if k_2 is positive and certainly dynamically stable if k_1 is zero or less than zero. If k_1 is positive, then it is possible for the oscillation amplitude to increase with decreasing altitude. This may be conveniently shown from the approximate equation (15e) for the envelope value of α. Writing this equation in the form

$$\left(\frac{\alpha}{\alpha_E}\right)^* = \frac{1}{\sqrt{\pi\sqrt{k_2}}}\ e^{\left(k_1 e^{-\beta y} + \frac{\beta y}{4}\right)} \qquad\qquad (30)$$

we find that the derivative of this function with respect to y is zero when

$$k_1 e^{-\beta y} = \frac{1}{4}$$

or

$$y = \frac{1}{\beta}\ln(4k_1) \qquad\qquad (31)$$

Thus if positive k_1 is even as large as 0.25, the analysis indicates that the incipience of divergence occurs (at sea level). For larger positive values serious divergence at the lower altitudes would be anticipated. In order to obtain a better grasp of the nature of such motions it is instructive to examine the indicated behavior of a missile with some arbitrarily assumed (but practicably realizable) static stability for several values of k_1. For this purpose let it be supposed that k_2 is 10^4 and k_1 has, in turn, the value -10, 0, and +10. The equation (15e)

then yields the envelope curve of angular history shown in figure 1. It
is indicated that positive values of k_1 could promote serious divergence
of the amplitude of angular oscillation. Friedrich and Dore (ref. 2) dis-
cussed the possibility of such divergence and noted that these adverse
effects could occur if the missile underwent large reductions in speed
during the descent. However, no consideration was given in their report
to the importance of the damping terms. In other words what they con-
sidered, in the language of this report, was that the coefficient k_1 (as
given by eq. (10c)) was overwhelmingly influenced by the drag coefficient.
These results of their analysis thus imply that high drag shapes are unsat-
isfactory for ballistic missile application in spite of their inherent
advantages in the aerodynamic heating problem (see, e.g., ref. 1).

The question of importance is, then, whether or not it is realistic
to ignore the damping terms (C_{L_α}) and $(C_{m_q} + C_{m_{\dot\alpha}})$ due to plunging and
rotation, respectively, in the determination of sign and magnitude of
k_1. To answer this question it is convenient to consider a simple conical
shape of arbitrary cone half-angle, δ.

To investigate the sign of k_1 for cones it is sufficient to
evaluate the "dynamic stability" factor

$$C_D - C_{L_\alpha} + (C_{m_q} + C_{m_{\dot\alpha}})\left(\frac{l}{\sigma}\right)^2$$

in equation (10c) by use of the relations of equations (28a) and (28b).
This has been done and the results are presented in figure 2 for several
center-of-gravity positions. (Note that $l_{cg}/l = 3/4$ is the center of
volume and a most likely position for the center of gravity.) From fig-
ure 2 it is seen that k_1 must always be negative for conical (and pre-
sumably for near conical) shapes. Thus the inference of reference 2 that
high-drag (i.e., large δ) shapes are necessarily undesirable from the
dynamic stability viewpoint is unjustified. Nevertheless, it should be
noted that while for the high-drag cones previously discussed the value
of k_1 was always negative, high-drag shapes which are blunted at the
nose can, in fact, have positive values of k_1. This leads to some concern
since, for reasons of aerodynamic heating, considerable blunting of the
nose may be desirable. However, it should be noted that the divergences
indicated by the analysis given previously are greater than what will
actually occur for the following reason: The analysis employs the velocity-
altitude relations from reference 1 and so does not include the effect of
gravity on the velocity-altitude history. This assumption is admissible
for the high-speed portions of the trajectory and for the portions wherein
the deceleration is large compared to that of gravity. For low drag shapes
the assumption is generally admissible over the whole altitude range but

for high drag shapes it becomes inadmissible at low altitudes. Thus the actual trajectory is not a linear one but is steepened at the low altitudes and the actual velocity approaches the so-called "terminal velocity" (i.e., that speed for which the drag equals the weight) rather than zero velocity. Then, in actuality the term $(dV/dy)/V$ in equation 7(a) approaches zero rather than the value indicated by equation 8(c). Hence, while at high altitudes k_1 is determined by the "dynamic stability" factor given above, at low altitudes for high drag shapes it would be determined more nearly by

$$-C_{L_\alpha} + (C_{m_q} + C_{m_{\dot\alpha}})\left(\frac{l}{\sigma}\right)^2$$

and thus the actual value of k_1 at low altitudes would be more negative than the analysis would indicate. Therefore, while divergence of the motion might occur for a high drag shape, it would not necessarily continue.

Next it is in order to examine the sign of the factor which controls the static stability parameter

$$k_2 = \frac{\rho_0 A}{2\beta^2 m \sin^2\theta_E}\left[-C_{m_\alpha}\left(\frac{l}{\sigma^2}\right) + C_{L_\alpha}\beta \sin \theta_E\right]$$

It is shown in Appendix D that the second term in the bracketed expression is small compared to the first for practical cases so that it is only necessary to be assured that C_{m_α} is negative to insure stability. In

figure 3 the Newtonian value of $C_{m_\alpha}\left(\frac{l}{\sigma}\right)^2$ (from eqs. (28a) and (28b)) is

plotted as a function of δ for various values of l_{cg}/l, and it is seen
that when δ is small, care must be exercised to keep the center of gravity
far forward. It should be noted (see ref. 9) that the center of pressure
is independent of Mach number down to the Mach number of shock detachment.
Thus the hypersonic requirement of l_{cg} is also the supersonic requirement.

From the preceding discussion, it is apparent that at least from low
supersonic to hypersonic speeds, positive static stability (i.e., positive
k_2) can be obtained. Similarly, it can be shown that over the same speed
range dynamic stability is assured (i.e., negative k_1). Now it is impor-
tant to determine the magnitude of the static and dynamic stability which
can be provided. To this end the following digression in the discussion
is in order.

For long-range ballistic missiles the aerodynamic heating problem
must be the principal consideration in design. It has been shown (e.g.,
see ref. 1) that, generally, the aerodynamic heating problems are
reduced when the value of k_0 is increased. On the other hand, if k_0
is too large then the speed of descent of the missile becomes low for too
great a part of the final trajectory which increases the vulnerability of
the missile. Thus some compromise is required and this compromise value
of k_0 tends to be larger the longer the range. A value that will be
considered herein to be a reasonable one for a 3,000- to 5,000-mile range
would be of the order of 5 to 20.

Now, k_1 (see eqs. (8b) and (10c)) can be written in terms of k_0 in
the form

$$k_1 = \frac{k_0}{4}\left[1 - \frac{C_{L_\alpha}}{C_D} + \left(\frac{C_{m_q} + C_{m_{\dot\alpha}}}{C_D}\right)\left(\frac{l}{\sigma}\right)^2\right] \qquad (32a)$$

while for k_2, if the $C_{L_\alpha}\beta \sin \theta_E$ part is neglected (see Appendix D), this
parameter becomes

$$k_2 = -\frac{k_0}{2\beta l \sin \theta_E}\left(\frac{C_{m_\alpha}}{C_D}\right)\left(\frac{l}{\sigma}\right)^2 \qquad (32b)$$

Values of k_1/k_0 and $\beta l \sin \theta_E k_2/k_0$ are given in tables II and III. Since
k_1/k_0 depends upon the location of the center of gravity and the cone
angle while k_2/k_0 depends upon these factors and, in addition, the length
of the missile, it is necessary to consider some examples in order to
determine the magnitudes likely to be realistic for k_1 and k_2. Accord-
ingly, let it be assumed that the missile weight is 3,000 pounds, that the

entrance angle of the trajectory, θ_E, is 30°, and that the values of the atmospheric density relations are those of reference 1 ($\rho_0 = 0.0034$ slugs per cubic foot, $\beta^{-1} = 22,000$ feet). For values of k_0 equal, in turn, to 5, 10, and 20 the base diameters, lengths, and volumes of the example missiles are those given in figures 4(a), 4(b), and 4(c), respectively, as functions of cone half-angle. For this analysis it is arbitrarily assumed that the maximum allowable missile length is 30 feet and the minimum allowable volume is 10 cubic feet (corresponding to a high missile density of 300 pounds per cubic foot). Thus in figures 4 the curves extend only to the cone half-angles which correspond to these two limits (the small cone-angle limit corresponds to the maximum allowed length and the large cone-angle limit to the maximum allowed density). In addition, it is arbitrarily specified that the center of gravity in each case is at a distance from the apex (l_{cg}) where the local diameter is 2-1/2 feet. The resulting ratios of l_{cg}/l are shown in figure 4(d).

With these physical characteristics, the values of k_1 and k_2 are those of figures 5 and 6. It is seen that the dynamic stability is greatest for large values of the drag parameter but for small values of the cone angle. On the other hand, the static stability is generally greatest for large values of both the drag parameter and cone angle. A notable exception to this trend of the static stability parameter is the sharp decrease of k_2 at the largest angle for the $k_0 = 5$ case. This sudden reduction results from the fact that the center-of-gravity position has rather closely approached the center of pressure.

Consider, now, two extreme cases: first, the $k_0 = 5$ missile at maximum allowed density and second, the $k_0 = 20$ missile at maximum allowed length. The former has least values for both stability parameters and therefore will oscillate with the largest amplitudes, while the latter has the largest dynamic stability parameter and has a rather high value for the static stability parameter and thus should be representative of the opposite extreme. The angular behavior with altitude for these two missiles has been calculated using equations (15c) and (15e) and is shown in figures (7a) and (7b). The high altitude oscillations of figure 7(a) are similar to those of (7b) but displaced downward, altitudewise, by about 25,000 feet. This is an effect of the lower static stability parameter for the $k_0 = 5$ missile. At the lower altitudes the $k_0 = 20$ missile oscillations decrease more rapidly by virtue of the larger dynamic stability parameter.

<div align="center">Heating</div>

It was pointed out in the Introduction of this report that when the time rates of aerodynamic heating are largest, it is important that the oscillation amplitudes be small in order that additional coolant mass will not be required to protect the vehicle from excessive local heating. It

is to be expected that, at least for not-too-small cone angles, maximum oscillation amplitudes of the order of a few degrees of arc should be permissible with no important adverse effects.

To determine whether or not the oscillations will be important as regards aerodynamic heating it is again convenient to consider a particular example. The same 3,000-pound missiles are used in this study. Since the laminar heating rate always reaches a maximum at a higher altitude than does the maximum for turbulent heating, it follows that $(\alpha/\alpha_E)^*$ at maximum heating will be greater in the laminar case. The amplitude ratio at the altitude for maximum laminar heating rate (calculated using eq. (19d)) is shown for the example missiles in figure 8. It is seen that these values are so low that no complications of the maximum heating rate problem due to initial angular misalignment with the flight path, α_E, should be expected. In figure 9 both the angular amplitude ratio and the ratio of laminar heating rate to maximum laminar heating rate (see ref. 1) are plotted as a function of altitude for one particular example ($k_O = 5$, $\delta = 25^O$), which shows that while the amplitude ratio is very small at the altitude for which maximum heating occurs, it may become sufficiently important at the higher altitudes where the heating rate is still fairly high to require consideration in design.

Loads

To show the degree to which lateral loads due to α_E are important it is again useful to consider the example missiles considered earlier. To evaluate the maximum normal force using equation (21c) it is necessary to specify the entrance speed, V_E, and it will be assumed, for the examples, that the speed is 20,000 feet per second. The maximum normal forces in terms of missile weight per degree angle misalignment at atmospheric entrance for the examples are shown in figure 10. While the normal forces are increased for the longer missiles (due to increased surface area), it does not appear that they could be too serious in a practical case. A 20° value for α_E only promotes a 3g normal acceleration for the long missiles which is small compared to the deceleration due to drag which (from the analysis of ref. 1) is 51g. Moreover, the maximum normal loads are not additive to the maximum drag loads since, as seen in figure 11, they occur at different altitudes.

Miss Distance

Before considering the actual magnitudes of the miss distances due to α_E or α_T it is well to discuss the accuracy of the analysis of miss distance given previously. In the analysis it is assumed that the velocity at all points of the trajectory is given by the exponential expression of

equation (8a) and this expression was, in turn, obtained by neglecting the
effect of gravity. As noted earlier the neglect of the effect of gravity
is unimportant in the evaluation of the velocity-altitude history except
when the velocity is low and, simultaneously, the deceleration due to
drag becomes comparable to the acceleration of gravity. Then the velocity
given by the analysis falls below that which would actually occur. In
the analysis of miss distance it should be clear that the miss distance
increases rapidly as the velocity decreases, and, hence, the miss distances
given by the analysis are in error by an amount which increases rapidly
with increasing k_O when the decelerations near $y = 0$ become of the order
of the acceleration of gravity. To assure that the deceleration at sea
level is not less than 1g, it is required (from ref. 1) that

$$k_O e^{-k_O} \leqq \frac{2g}{V_E{}^2 \beta \sin \theta_E}$$

For example, for an entrance speed of 20,000 feet per second and for
$\theta_E = 30^O$, the sea level deceleration reaches 1g for k_O of about 7 (see
ref. 1); hence, the values of $F(k_O,k_1,k_2)$ (see Appendix C) and $F_1(k_O)$
from table I should not be used, under these conditions, for values of
k_O in excess of about 7, particularly as k_O greatly exceeds this value.
Thus in the calculations to follow the miss distances for $k_O = 20$ are not
included and, in addition, the reader must note that even for $k_O = 10$ the
estimated miss distances exceed the actual ones.

The range target errors per degree angle misalignment at atmospheric
entrance for the example missiles ($V_E = 20,000$ ft/sec, $\theta_E = 30^O$) are shown
in figure 12. The deflection target error, not shown, is simply one-half
the range value. It is seen that, as with the normal force, the miss
distance is greatest for the smallest cone angles. However, the miss dis-
tance is trivial since even for an α_E of say 20° the range target error
is but about 20 feet in the worst case.

A serious problem is the miss distance which will result from a trim
angle even slightly different than zero. In figure 13 is shown the range
target error per degree of trim angle for the k_O of 5 and 10. It is
seen that a trim angle of as little as 0.1^O can cause a range error of
many miles. As the cone angle increases then for a given value of k_O,
the miss distance diminishes until when the cone half-angle is 45° the
miss distance is zero since the lift-curve slope is then zero (see
eq. (27a)). Except in this special case, however, the miss distance due
to even a slight trim angle is very important. One method for reducing
this miss distance would be to spin the missile about its axis so that
it would follow a corkscrew path during descent. This solution introduces
another difficulty, however, in that care may have to be taken to keep the
spin rate from approaching the pitching (or yawing) frequency else tumbling
may occur if the missile is not identical as regards aerodynamic and

inertial characteristics about any radial axis (see ref. 5 or 10).
Unfortunately, the pitching frequency varies from zero to the maximum
value given by equation (16). The maximum frequencies for the example
missiles are shown in figure 14. One obvious way to avoid tumbling
resulting from "roll coupling" would be to spin the missile at a rate
which exceeds, by a good margin, the maximum shown in figure 14. If the
spin rates were the maximum pitch rates, the rim speeds at the base (i.e.,
at maximum diameter) would be those shown in figure 15. Since the required
spin rate would have to materially exceed this rate, it is clear that a
serious stress problem due to centrifugal loading might result (especially
for small cone angles). In consequence, a better solution might be to
spin the missile at a rate which is always less than the value of the
pitch frequency at any given altitude, but the difficulty, then, would
be one of assuring that the spin rate could not accidentally approach the
pitch frequency. In the preceding discussion it has been tacitly assumed
that the missile is not identical as regards the aerodynamic and inertial
characteristics about any radial axis so that the spin rate must not at
any time match the pitch rate. Since the pitch rate changes rapidly with
time (particularly at the higher altitudes), it is probably not a justi-
fiable requirement that the spin rate not ever be the pitch rate, particu-
larly since the asymmetries which exist may be trivial. Some further
consideration must clearly be given this problem.

Effect of Initial Tumbling

In the discussion to this point it has been assumed that the missile
enters the atmosphere misaligned by an arbitrary but fixed angle with
respect to the flight path. When the missile is actually tumbling before
entering the atmosphere, then the analysis given previously cannot be used
since the equation of motion is restricted to small-angle considerations.
(That the analysis is inadmissible is reflected in the fact that if, in

equation (13), C_2 has a value which is not zero, then $C_2 Y_0 \left(2 \sqrt{k_2 + k_1} \ e^{-\frac{\beta y}{2}} \right)$

becomes infinite if y is infinite.) In spite of this deficiency, some
general remarks can be made about the effect of initial tumbling. It is
clear at the outset that the missile must have but one possible trim
attitude if initial tumbling occurs. If not, it could descend at some
attitude for which no adequate protection for aerodynamic heating and
loading had been provided. Furthermore it is a requirement that it must
be righted to about the correct attitude at an altitude which is suffi-
ciently high that the angular motions will become small by the time the
heating and loading are intense. One obvious way which might assure that
these conditions will be met would be to dispose of the empty fuel and
oxidizer tankage only after the missile has entered the atmosphere
sufficiently far to adequately correct the attitude.

CONCLUSIONS

From an analysis of the motion of a ballistic missile initially mis-
aligned with respect to the flight path prior to the entry into the
atmosphere, it is concluded that it is possible to:

1. Provide a continuously damped oscillation history with descent
through the atmosphere.

2. Keep the oscillations to a small amplitude when at altitudes for
which aerodynamic heating and loading are severe.

3. Prevent excessively large loads due to the oscillating motion.

Moreover, while the miss distance at the target due to the initial
misalignment angle is trivial, the error that can occur due to the trim
angle being even slightly different than zero can be very large and its
effect must be minimized in some manner.

Since tumbling may occur prior to entry into the atmosphere the mis-
sile must have only one trim attitude and must be brought near this attitude
before the missile has progressed too far down through the atmosphere.

Ames Aeronautical Laboratory
    National Advisory Committee for Aeronautics
        Moffett Field, Calif., June 15, 1956

APPENDIX A

SYMBOLS

a   constant (See Appendix C, eqs. (C2).)

A   reference area for coefficient evaluation (base area
             for cones)

b   constant (See Appendix C, eqs. (C2).)

c   constant (See Appendix C, eqs. (C2).)

C_1,C_2 constants of integration

C_D drag coefficient

C_{L_α} rate of change of lift coefficient with angle of
             attack, $\left(\dfrac{\partial C_L}{\partial \alpha}\right)_{\alpha \to 0}$

C_{m_α} rate of change of moment coefficient with angle of
             attack, $\left(\dfrac{\partial C_m}{\partial \alpha}\right)_{\alpha \to 0}$

$C_{m_{\dot\alpha}}$ change of moment coefficient with time rate of change
             of angle of attack, $\dfrac{\partial C_m}{\partial\left(\dot\alpha \dfrac{l}{V}\right)_{\dot\alpha \to 0}}$

C_{m_q} rate of change of moment coefficient with angular
             velocity, $\dfrac{\partial C_m}{\partial\left(q \dfrac{l}{V}\right)_{q \to 0}}$

C_{N_α} rate of change of normal-force coefficient with angle
             of attack, $\dfrac{\partial C_N}{\partial \alpha_{\alpha \to 0}}$

C_X axial-force coefficient

d	diameter of body base
e	Naperian base
$f_1(t), f_2(t)$	functions of time
$f_3(y), f_4(y)$	functions of altitude
$F_1(k_0)$	function used in evaluating of "miss distance" due to α_T (See table I.)
$F(k_0, k_1, k_2)$	function used in evaluation of "miss distance" due to α_E (See Appendix C.)
g	acceleration due to gravity
h	integer (See Appendix C.)
I	mass moment of inertia
$I_{0,1,2,...}$	integrals (See Appendix C.)
$J_0(\ )$	Bessel function of the first kind of zero order
$J_{1,2,3,...,r,s}(\ )$	Bessel function of the first kind of order $1,2,3,...,r,s$
k_0	the "drag" parameter (See eq. (8b).)
k_1	the "dynamic stability" parameter (See eq. (10c).)
k_2	the "static stability" parameter (See eq. (10c).)
k_3	the "cross-products" parameter (See eq. (10c).)
l	body length and reference length for moment coefficient evaluation
l_{cg}	distance from body bow to center of gravity
L	cross-wind force
m	missile mass
n	distance normal to the trajectory the missile would have if it were angularly aligned with flight path and without angular velocity
N	normal force (force perpendicular to the axis of revolution)

$P_{1,2,3,\ldots,r,s}(\ )$ functions (See Appendix C.)

q angular velocity

r integer (See Appendix C.)

s integer (See Appendix C.)

$S_{0,1,2,\ldots,r,s}(\ )$ functions (See Appendix C.)

t time

V speed at arbitrary altitude

V_E speed on entry to the atmosphere

x along range distance

y altitude

Y dimensionless altitude, βy

$Y_0(\ )$ Bessel function of second kind of zero order

z across range distance

α angle of attack

α_E angle of attack on entry to the atmosphere

α_T angle of trim

β density exponential (See eq. (1).)

δ half-angle of cone

$\left(\epsilon_{\alpha_E}\right)_z$ deflection target error due to α_E

$\left(\epsilon_{\alpha_E}\right)_x$ range target error due to α_E

$\left(\epsilon_{\alpha_T}\right)_z$ deflection target error due to α_T

$\left(\epsilon_{\alpha_T}\right)_x$ range target error due to α_T

ζ altitude variable (See eq. (23b).)

η angle-of-attack function (See eq. (11).)

θ_E angle between flight path and earth's surface that missile has on entering the atmosphere

ρ air density

ρ_0 air density at sea level

σ radius of gyration

ψ an arbitrary variable (See Appendix B.)

ω oscillation frequency

Superscripts

$(\ )^*$ maximum value of the bracketed parameter which occurs in any particular cycle of oscillation

Subscripts

$(\ )_{max}$ maximum value of the bracketed parameter

Except for the parameters C, f, F, and k:

$(\ )_1$ value of the bracketed parameter at altitude for maximum deceleration

$(\ )_2$ value of the bracketed parameter at altitude for maximum turbulent heat-transfer rate

$(\ )_3$ value of the bracketed parameter at altitude for maximum laminar heat-transfer rate

$(\ )_4$ value of the bracketed parameter at altitude for maximum normal force

APPENDIX B

DETERMINATION OF ANGULAR VELOCITY AND ANGULAR ACCELERATION

It is the purpose in this appendix to derive the expressions for the angular velocity and acceleration from equation (15b) which gives the angular displacement as a function of altitude. Noting that

$$\frac{dJ_0(\psi)}{dy} = -J_1(\psi) \frac{d\psi}{dy}$$

then differentiation of equation (15b) yields

$$\frac{d(\alpha/\alpha_E)}{dy} = -k_1\beta e^{-\beta y} e^{k_1 e^{-\beta y}} J_0\left(2\sqrt{k_2 + k_1}\ e^{-\frac{\beta y}{2}}\right) +$$

$$\frac{\beta}{2} e^{k_1 e^{-\beta y}}\left[2\sqrt{k_2 + k_1}\ e^{-\frac{\beta y}{2}}\ J_1\left(2\sqrt{k_2 + k_1}\ e^{-\frac{\beta y}{2}}\right)\right] \qquad \text{(B1)}$$

and further noting that

$$\frac{d}{dy}\left[\psi J_1(\psi)\right] = \psi J_0(\psi) \frac{d\psi}{dy}$$

then

$$\frac{d^2(\alpha/\alpha_E)}{dy^2} = \beta^2 e^{k_1 e^{-\beta y}}\left(k_1{}^2 e^{-2\beta y} - k_2 e^{-\beta y}\right) J_0\left(2\sqrt{k_2 + k_1}\ e^{-\frac{\beta y}{2}}\right) -$$

$$2\beta^2 k_1 \sqrt{k_2 + k_1}\ e^{-\frac{3\beta y}{2}}\ e^{k_1 e^{-\beta y}} J_1\left(2\sqrt{k_2 + k_1}\ e^{-\frac{\beta y}{2}}\right) \qquad \text{(B2)}$$

Using equations (5a), (8a), and (B1)

$$\frac{d(\alpha/\alpha_E)}{dt} = \beta V_E \sin \theta_E e^{\left(k_1 - \frac{k_0}{2}\right)e^{-\beta y}}\left[k_1 e^{-\beta y}J_0\left(2\sqrt{k_2 + k_1}\ e^{-\frac{\beta y}{2}}\right) - \sqrt{k_2 + k_1}\ e^{-\frac{\beta y}{2}}J_1\left(2\sqrt{k_2 + k_1}\ e^{-\frac{\beta y}{2}}\right)\right]$$

(B3)

and using equations (5b), (8a), (B1), and (B2)

$$\frac{d^2(\alpha/\alpha_E)}{dt^2} = \beta^2 V_E^2 \sin^2\theta_E e^{(k_1 - k_0)e^{-\beta y}}\left\{\left[\left(k_1^2 - \frac{k_1 k_0}{2}\right)e^{-2\beta y} - k_2 e^{-\beta y}\right]J_0\left(2\sqrt{k_2 + k_1}\ e^{-\frac{\beta y}{2}}\right) - \left(2k_1 - \frac{k_0}{2}\right)\sqrt{k_2 + k_1}\ e^{-\frac{3\beta y}{2}}J_1\left(2\sqrt{k_2 + k_1}\ e^{-\frac{\beta y}{2}}\right)\right\}$$

(B4)

Since, for the cases of usual interest, the coefficient k_2 is so very large compared to k_1 then one may use the approximate expressions

$$\frac{d(\alpha/\alpha_E)}{dt} = -\sqrt{k_2}\ \beta V_E \sin \theta_E e^{-\frac{\beta y}{2}}e^{\left(k_1 - \frac{k_0}{2}\right)e^{-\beta y}}J_1\left(2\sqrt{k_2}\ e^{-\frac{\beta y}{2}}\right)$$

(B5a)

which, for large values of the argument becomes

$$\frac{d(\alpha/\alpha_E)}{dt} = -\sqrt{\frac{\sqrt{k_2}}{\pi}}\ \beta V_E \sin \theta_E e^{-\frac{\beta y}{4}}e^{\left(k_1 - \frac{k_0}{2}\right)e^{-\beta y}}\cos\left(\frac{3\pi}{4} - 2\sqrt{k_2}\ e^{-\frac{\beta y}{2}}\right)$$

(B5b)

so that the maximum angular velocity during a cycle is

$$\left[\frac{d(\alpha/\alpha_E)}{dt}\right]^* = \sqrt{\frac{\sqrt{k_2}}{\pi}}\,\beta V_E \sin\theta_E e^{-\frac{\beta y}{4}} e^{\left(k_1 - \frac{k_0}{2}\right)e^{-\beta y}} \tag{B5c}$$

Similarly, since k_2 is very large compared to $\sqrt{k_2}$ or k_1 then approximately

$$\frac{d^2(\alpha/\alpha_E)}{dt^2} = -k_2\beta^2 V_E^2\sin^2\theta_E e^{-\beta y}e^{(k_1-k_0)e^{-\beta y}}J_0\!\left(2\sqrt{k_2}\,e^{-\frac{\beta y}{2}}\right) \tag{B6a}$$

which for large values of the argument becomes

$$\frac{d^2(\alpha/\alpha_E)}{dt^2} = -\frac{k_2^{\frac{3}{4}}}{\sqrt{\pi}}\,\beta^2 V_E^2\sin^2\theta_E e^{-\frac{3\beta y}{4}}e^{(k_1-k_0)e^{-\beta y}}\cos\!\left(\frac{\pi}{4} - 2\sqrt{k_2}\,e^{-\frac{\beta y}{2}}\right) \tag{B6b}$$

and the maximum angular acceleration during a cycle is

$$\left[\frac{d^2(\alpha/\alpha_E)}{dt^2}\right]^* = \frac{k_2^{\frac{3}{4}}}{\sqrt{\pi}}\,\beta^2 V_E^2\sin^2\theta_E e^{-\frac{3\beta y}{4}}e^{(k_1-k_0)e^{-\beta y}} \tag{B6c}$$

APPENDIX C

NUMERICAL INTEGRATION METHOD FOR THE INTEGRAL $F(k_0,k_1,k_2)$

The following method for the numerical solution of the function $F(k_0,k_1,k_2)$ was devised by Dr. William Mersman of Ames Aeronautical Laboratory. The integral to be evaluated is, from equation (24a),

$$k_2 F(k_0,k_1,k_2) = \int_0^a \frac{e^{b\zeta^2}}{\zeta} I_0(\zeta,c)d\zeta \qquad (C1)$$

where

$$\left.\begin{array}{l} a = 2\sqrt{k_2} \\[2mm] b = k_0/8k_2 \\[2mm] c = \left(\dfrac{1}{2}k_0 - k_1\right)/4k_2 \end{array}\right\} \qquad (C2)$$

and

$$I_0(\zeta,c) = \int_0^\zeta e^{-c\zeta_1^2} \zeta_1 J_0(\zeta_1)d\zeta_1 \qquad (C3)$$

By reference 7, page 45,

$$\zeta_1^{r+1} J_r(\zeta_1) = \frac{d}{d\zeta_1}\left[\zeta_1^{r+1} J_{r+1}(\zeta_1)\right], \qquad r = 0,1,2,\ldots \qquad (C4)$$

Introducing

$$I_r(\zeta,c) \equiv \int_0^\zeta e^{-c\zeta_1^2} \zeta_1^{r+1} J_r(\zeta_1)d\zeta_1, \qquad r = 0,1,2,\ldots \qquad (C5)$$

an integration by parts gives the recursion formula

$$I_r(\zeta,c) = e^{-c\zeta^2}\zeta^{r+1}J_{r+1}(\zeta) + 2c\int_0^{\zeta} e^{-c\zeta_1^2}\zeta_1^{r+2}J_{r+1}(\zeta_1)$$

That is,

$$I_r(\zeta,c) = e^{-c\zeta^2}\zeta^{r+1}J_{r+1}(\zeta) + 2cI_{r+1}(\zeta,c) , \qquad r = 0,1,2 \qquad (C6)$$

If this equation is multiplied by $(2c)^{r-s}$ and then summed on r from s to infinity, the following series representation is obtained

$$I_s(\zeta,c) = e^{-c\zeta^2}\zeta^{s+1}\sum_{h=0}^{\infty}(2c\zeta)^h J_{s+h+1}(\zeta) \qquad (C7)$$

for any $s = 0,1,2,. . .$, the series being convergent provided that $|2c\zeta| < |$.

In particular, then, setting $s = 0$ gives

$$I_0(\zeta,c) = e^{-c\zeta^2}\zeta\sum_{h=0}^{\infty}(2c\zeta)^h J_{h+1}(\zeta)$$

and substitution in equation (C1) gives

$$k_2F(k_0,k_1,k_2) = \sum_{s=0}^{\infty} S_s(a,b,c) \qquad (C8)$$

where

$$S_s(a,b,c) = (2c)^s\int_0^a e^{-(c-b)\zeta^2}\zeta^s J_{s+1}(\zeta)d\zeta , \qquad s = 0,1,2,. . . \qquad (C9)$$

the series is convergent if $|2ca| < |$.

Consider, first, the term s = 0

$$S_0(a,b,c) = \int_0^a e^{-(c-b)\zeta^2} J_1(\zeta) d\zeta$$

By reference 7, page 18, $J_1(\zeta) = -dJ_0(\zeta)/d\zeta$. Hence integration by parts gives

$$S_0(a,b,c) = J_0(0) - e^{-(c-b)a^2} J_0(a) - 2(c-b) \int_0^a e^{-(c-b)\zeta^2} \zeta J_0(\zeta) d\zeta$$

Referring to equation (C3), this is, since $J_0(0) = 1$,

$$S_0(a,b,c) = 1 - e^{-(c-b)a^2} J_0(a) - 2(c-b)I_0(a,c-b) \tag{C10}$$

To obtain a recursion formula for the general S_s, substitute in equation (C9) the equation

$$J_{s+1}(\zeta) = \frac{2s}{\zeta} J_s(\zeta) - J_{s-1}(\zeta)$$

from reference 7, page 45. This gives immediately

$$S_s(a,b,c) = 4csS_{s-1}(a,b,c) - (2c)^s I_{s-1}(a,c-b) , \quad s = 1,2,3,\ldots \tag{C11}$$

Thus, equations (C8), (C10), and (C11) reduce the problem to one of computing the sequence $I_s(a,c-b)$, s = 0,1,2,. . . .

For computing purposes, it is desirable to introduce slowly varying quantities. The following substitution turns out to be convenient

$$P_r(a,c-b) = e^{+(c-b)a^2} I_r(a,c-b)/a^{r+1} \quad r = 0,1,2,\ldots \tag{C12}$$

The computing problem is then summarized by the following formulae:

$$P_s(a,c-b) = \sum_{h=0}^{\infty} [2a(c-b)]^h J_{s+h+1}(a) \qquad (C13)$$

for any $s = 0,1,2,\ldots$

$$P_r(a,c-b) = J_{r+1}(a) + 2a(c-b)P_{r+1}(a,c-b) , \qquad r = 0,1,2,\ldots \quad (C14)$$

$$S_0(a,b,c) = 1 - e^{-(c-b)a^2}[J_0(a) + 2a(c-b)P_0(a,c-b)] \qquad (C15)$$

$$S_s(a,b,c) = 4csS_{s-1}(a,b,c) - (2ca)^s e^{-(c-b)a^2}P_{s-1}(a,c-b) , \qquad s = 1,2,3,\ldots$$
$$(C16)$$

$$k_2 F(k_0,k_1,k_2) = \sum_{s=0}^{\infty} S_s(a,b,c) \qquad (C8)$$

The order in which the computations are to be performed is dictated by the following inequalities, each of which is obvious from the corresponding integral definition, under the following general assumptions

$$b \geqq 0 , \quad c \geqq 0 , \quad c-b \geqq 0$$

$$2ca < 1 , \quad 2a(c-b) < 1$$

The inequalities are

$$|P_s(a,c-b)| \leqq \frac{1}{1 - 2a(c-b)} , \qquad s = 0,1,2,\ldots \qquad (C17)$$

$$|S_s(a,b,c)| \leqq \frac{a}{s + 1} (2ac)^s , \qquad s = 0,1,2 \qquad (C18)$$

From the latter, it can be determined how many terms of the series (C8) are needed for any desired accuracy, so that (C8) is replaced in practice by

$$k_2 F(k_0, k_1, k_2) = \sum_{s=0}^{K} S_s(a, b, c) \tag{C19}$$

In the present work $K = 20$, giving a truncation error of less than 10^{-10}. Once K is chosen, P_K is obtained from equation (C13) with $s = K$ where again enough terms are taken to insure the desired accuracy. In the present work the computer automatically continued the series (C13) until the summand $[2a(c-b)]^h J_{K+h+1}(a)$ became less than 10^{-9}. Once P_K has been obtained from the series (C13), the recurrence relations (C14) are used to compute $P_{K-1}, P_{K-2}, \ldots P_1, P_0$ in that order. Then S_0 is computed from equation (C15), and $S_1, S_2, \ldots, S_K$ in that order from equation (C16).

In the present paper the significant range of parameters is

$$0 \leq k_0 \leq 10$$

$$-80 \leq k_1 \leq 0$$

$$5 \times 10^4 \leq k_2 \leq 8 \times 10^5$$

For this range it can be shown that the series (C19) can be truncated at $K = 1$ with an error less than 1×10^{-6}. Furthermore, in the expression for S_0 and S_1, equations (C15) and (C16), the terms involving the exponential function are also less than 1×10^{-6}. This gives the simple approximate formulae

$$S_0 = 1 , \quad S_1 = 4c$$

and, hence

$$F(k_0, k_1, k_2) = \frac{1}{k_2} \left[1 + \frac{\frac{1}{2} k_0 - k_1}{k_2} \right] \tag{C20}$$

with an error less than $2 \times 10^{-6} / k_2$.

APPENDIX D

ORDER OF MAGNITUDE OF FACTORS AFFECTING STABILITY

In the analysis of this report, a number of simplifying assumptions were made regarding the relative importance of the several factors which influence the stability. It is the purpose herein to demonstrate that three of the assumptions which are of particular importance are, in fact, justified. These assumptions are:

(1) In the evaluation of values of k_2 (eq. (10c)) it is permissible to ignore the C_{L_α} contribution in comparison with the C_{m_α} contribution. (This assumption is desired but not required.)

(2) In terms involving $k_2 + k_1$, that k_1 is unimportant. (This assumption is desired but not required.)

(3) That $k_3 - k_1{}^2$ is trivial in comparison with $k_2 + k_1$ (or, from assumption (2), in comparison with k_2). (This assumption is required to obtain the solution for the fundamental differential equation of motion (eq. (12).)

It is to be noted at the outset that k_1, k_2, and k_3 can be written in terms of the drag parameter, k_0, in the forms

$$k_1 = \frac{k_0}{4}\left[1 - \frac{C_{L_\alpha}}{C_D} + \left(\frac{C_{m_q} + C_{m_{\dot\alpha}}}{C_D}\right)\left(\frac{l}{\sigma}\right)^2\right] \tag{D1}$$

$$k_2 = \frac{k_0}{2\beta l \sin\theta_E}\left[-\left(\frac{C_{m_\alpha}}{C_D}\right)\left(\frac{l}{\sigma}\right)^2 + \left(\frac{C_{L_\alpha}}{C_D}\right)\beta l \sin\theta_E\right] \tag{D2}$$

$$k_3 = \frac{k_0{}^2}{4}\left[-\frac{C_{L_\alpha}}{C_D} - \left(\frac{C_{m_q}C_{L_\alpha}}{C_D{}^2}\right)\left(\frac{l}{\sigma}\right)^2\right] \tag{D3}$$

The demonstration of the validity of the assumptions (1), (2), and (3) will be considered in the sections I, II, and III as follow for conical shapes.

I. For this demonstration it is necessary to show that

$$\left(\frac{C_{L_\alpha}}{C_D}\right)\beta l \sin \theta_E$$

is trivial in comparison with

$$- \frac{C_{m_\alpha}}{C_D}\left(\frac{l}{\sigma}\right)^2$$

Since the C_{L_α} term is larger the larger the value of l and $\sin \theta_E$, it will be assumed that the θ_E is about (slightly greater than) 45° and the length is that for a 6-foot diameter base (i.e., $l = (3/\tan \delta)$ ft). Then (since $\beta^{-1} = 22{,}000$ ft) the comparison of the components is between, approximately

$$\frac{C_{L_\alpha}\times 10^{-4}}{C_D \tan \delta}$$

and

$$- \frac{C_{m_\alpha}}{C_D}\left(\frac{l}{\sigma}\right)^2$$

Assuming l_{cg}/l is 0.30, 0.50, and 0.70 then the ratio of the exact value of k_2 to the approximate value of k_2 obtained by ignoring the C_{L_α} term is that shown in figure 16. It is seen that the approximation is excellent except when C_{m_α} goes to zero (shown for the $l_{cg} = 0.70$ case). Of course, in no practical case would C_{m_α} be allowed to approach zero.

II. To show that k_1 is trivial in comparison with k_2 it is necessary to show that

$$\frac{k_1}{k_0} = \frac{1}{4}\left[1 - \frac{C_{L_\alpha}}{C_D} + \left(\frac{C_{m_q} + C_{m_{\dot\alpha}}}{C_D}\right)\left(\frac{l}{\sigma}\right)^2\right]$$

is small compared to

$$\frac{k_2}{k_0} = - \frac{1}{2\beta l \sin \theta_E}\left[- \frac{C_{m_\alpha}}{C_D}\left(\frac{l}{\sigma}\right)^2\right]$$

Again the quantity k_2 will be least compared to k_1 when $l \sin \theta_E$ is largest; hence, the length and angle assumption of section I is used so that the comparison will be between

$$\frac{k_1}{k_0} = \frac{1}{4}\left[1 - \frac{C_{L_\alpha}}{C_D} + \left(\frac{C_{m_q} + C_{m_{\dot\alpha}}}{C_D}\right)\left(\frac{l}{\sigma}\right)^2\right]$$

and

$$\frac{k_2}{k_0} = -\frac{\tan \delta}{2\times10^{-4}}\left(\frac{C_{m_\alpha}}{C_D}\right)\left(\frac{l}{\sigma}\right)^2$$

Assuming $l_{cg}/l = 0.30$, 0.50, and 0.70 then the ratio of the value $k_2 + k_1$ to the value k_2 is that shown in figure 17. It is seen again that, except when C_{m_α} goes to zero, the approximation is excellent.

III. In this demonstration it is necessary to show that

$$(k_3 - k_1{}^2)e^{-2\beta y} = k_0{}^2\left[\frac{k_3}{k_0{}^2} - \left(\frac{k_1}{k_0}\right)^2\right]e^{-2\beta y}$$

is trivial compared to

$$(k_2 + k_1)e^{-\beta y} \cong k_2 e^{-\beta y} = k_0\left(\frac{k_2}{k_0}\right)e^{-\beta y}$$

The test of this assumption is more severe when k_0 is largest and y is minimum, and again, when $l \sin \theta_E$ is largest. Using the largest k_0 to be expected, say 20, and the length and angle from section I, and for $y = 0$, the severe comparison is then between

$$k_3 - k_1{}^2 = 400\left[\frac{k_3}{k_0{}^2} - \left(\frac{k_1}{k_0}\right)^2\right]$$

and

$$k_2 = -\frac{\tan \delta}{10^{-5}}\left(\frac{C_{m_\alpha}}{C_D}\right)\left(\frac{l}{\sigma}\right)^2$$

Assuming $l_{cg}/l = 0.30$, 0.50, and 0.70, then the ratio of $(k_3-k_1^2)/k_2$ is that shown in figure 18. It is seen again that, except when C_{m_α} goes to zero, the approximation is excellent. Moreover since these coefficients enter the differential equation (12) multiplied by $e^{-2\beta y}$ and $e^{-\beta y}$, respectively, and these exponential values have, at altitude, the values

y, ft	$e^{-2\beta y}$	$e^{-\beta y}$
0	1.00	1.00
50,000	1.06×10^{-2}	1.03×10^{-1}
100,000	1.12×10^{-4}	1.06×10^{-2}
150,000	1.19×10^{-6}	1.09×10^{-3}
200,000	1.25×10^{-8}	1.12×10^{-4}
250,000	1.31×10^{-10}	1.15×10^{-5}

then the integrated influence of the term involving $k_3 - k_1^2$ must be trivial compared to the k_2 term.

REFERENCES

1. Allen, H. Julian, and Eggers, A. J., Jr.: A Study of the Motion and
        Aerodynamic Heating of Missiles Entering the Earth's Atmosphere at
        High Supersonic Speeds. NACA TN 4047, 1957 (Supersedes NACA
        RM A53D28).

2. Friedrich, Hans R., and Dore, Frank J.: The Dynamic Motion of a
        Missile Descending Through the Atmosphere. Jour. Aero. Sci.,
        vol. 22, no. 9, Sept. 1955, pp. 628-632, 638.

3. Oswald, Telford Wilbert: The Influence of Variable Air Density and
        Non-Linear Aerodynamic Characteristics on Dynamic Behavior at
        Supersonic Speeds. PhD. Thesis, Calif. Inst. Tech., 1951.

4. Oswatitsch, Klaus: Similarity Laws for Hypersonic Flow. Kungl.
        Tekniska Hogskölan, Stockholm Inst. for Flygteknik, Tech. Note 16,
        July 19, 1950.

5. Charters, A. C.: The Linearized Equations of Motion Underlying the
        Dynamic Stability of Aircraft, Spinning Projectiles, and Symmet-
        rical Missiles. NACA TN 3350, 1955.

6. Kamke, E.: Differentialgleichungen, Lösungsmethoden und Lösungen,
        Band 1 Gewohnliche Differentialgleichungen, 3 Aufl, Chelsea Pub.
        Co., 1948, p. 442.

7. Watson, G. N.: A Treatise on the Theory of Bessel Functions.
        Cambridge Univ. Press, 1944.

8. Jahnke, Eugen, and Emde, Fritz: Funktionentafeln mit Formeln
        und Kurven. B. G. Teubner Pub. Co., Leipzig and Berlin, 1938.

9. Tobak, Murray, and Wehrend, William R.: Stability Derivatives of
        Cones at Supersonic Speeds. NACA TN 3788, 1956.

10. Nicolaides, John D.: On the Free Flight Motion of Missiles Having
        Slight Configurational Asymmetries. BRL Rep. 858, Aberdeen Proving
        Ground, Md., June 1953.

TABLE I.- ERROR FUNCTION, $F_1(k_O)$, EQUATION (26d)

k_O	$F_1(k_O)$
0	0.500
1	.571
2	.659
3	.773
4	.921
5	1.116
6	1.376
7	1.728
8	2.208
9	2.873
10	3.800

Note: The values should not be used when k_O is such that

$$k_O e^{-k_O} \leqq \frac{2g}{V_E{}^2 \beta \sin \theta_E}$$

TABLE II.- DYNAMIC STABILITY PARAMETER, k_1/k_0, FOR CONES

δ, deg \ $\frac{l_{cg}}{l}$	0	0.1	0.2	0.3	0.4	0.5	0.6	0.7	0.8	0.9	1.0
5	-59.74	-59.31	-58.87	-58.52	-58.57	-59.91	-65.04	-77.59	-90.02	-90.13	-85.16
10	-14.61	-14.53	-14.46	-14.41	-14.46	-14.78	-15.84	-18.19	-20.46	-20.51	-19.59
15	-6.256	-6.247	-6.243	-6.254	-6.300	-6.434	-6.767	-7.373	-7.859	-7.813	-7.547
20	-3.339	-3.354	-3.376	-3.408	-3.457	-3.532	-3.638	-3.728	-3.696	-3.567	-3.454
25	-1.997	-2.024	-2.058	-2.102	-2.153	-2.206	-2.228	-2.151	-1.956	-1.769	-1.671
30	-1.276	-1.311	-1.353	-1.402	-1.456	-1.500	-1.493	-1.370	-1.139	-.9240	-.8060
35	-.8510	-.8910	-.9380	-.9930	-1.048	-1.088	-1.072	-.9510	-.7321	-.5144	-.3723
40	-.5856	-.6300	-.6818	-.7386	-.7950	-.8320	-.8170	-.7120	-.5238	-.3202	-.1654
45	-.4168	-.4645	-.5188	-.5770	-.6318	-.6668	-.6548	-.5702	-.4167	-.2380	-.0833
50	-.3102	-.3603	-.4157	-.4730	-.5245	-.5563	-.5482	-.4830	-.3631	-.2142	-.0708
55	-.2476	-.2986	-.3530	-.4070	-.4534	-.4810	-.4760	-.4277	-.3323	-.2194	-.0956
60	-.2183	-.2680	-.3188	-.3672	-.4067	-.4293	-.4265	-.3923	-.3272	-.2385	-.1388
65	-.2149	-.2604	-.3050	-.3450	-.3761	-.3934	-.3919	-.3691	-.3246	-.2622	-.1811
70	-.2317	-.2697	-.3046	-.3347	-.3567	-.3688	-.3682	-.3539	-.3259	-.2857	-.2357
75	-.2617	-.2886	-.3122	-.3313	-.3449	-.3520	-.3518	-.3439	-.3284	-.3057	-.2765

TABLE III.- STATIC STABILITY PARAMETER, $\beta_l \sin \theta_E (k_2/k_0)$, FOR CONES

δ, deg	0	0.1	0.2	0.3	0.4	0.5	0.6	0.7	0.8	0.9	1.0
5	73.00	81.00	90.35	100.7	110.1	110.9	76.65	-44.85	-203.6	-243.8	-211.9
10	18.28	20.34	22.74	25.46	28.06	28.79	21.73	-4.548	-40.56	-52.90	-48.03
15	8.145	9.090	10.21	11.50	12.82	13.48	11.27	1.992	-11.72	-18.24	-17.94
20	4.596	5.150	5.820	6.605	7.445	7.530	7.325	3.466	-2.837	-6.850	-7.715
25	2.951	3.322	3.774	4.315	4.914	5.405	5.255	3.533	.3680	-2.195	-3.267
30	2.051	2.320	2.649	3.046	3.492	3.889	3.939	3.148	1.481	-.1520	-1.111
35	1.504	1.708	1.956	2.255	2.591	2.899	3.004	2.636	1.804	.7140	-.0380
40	1.143	1.301	1.491	1.717	1.967	2.197	2.298	2.126	1.639	1.012	.4699
45	.8890	1.011	1.156	1.324	1.505	1.666	1.746	1.666	1.403	1.031	.6666
50	.6985	.7915	.9000	1.021	1.145	1.252	1.306	1.271	1.131	.9200	.6900
55	.5485	.6165	.6930	.7755	.8560	.9220	.9505	.9400	.8690	.7545	.6200
60	.4233	.4700	.5205	.5715	.6195	.6565	.6755	.6690	.6350	.5775	.5050
65	.3147	.3434	.3728	.4014	.4264	.4449	.4541	.4516	.4367	.4106	.3762
70	.2179	.2329	.2474	.2606	.2715	.2794	.2831	.2824	.2768	.2666	.2526
75	.1328	.1388	.1441	.1487	.1524	.1550	.1562	.1560	.1543	.1512	.1468
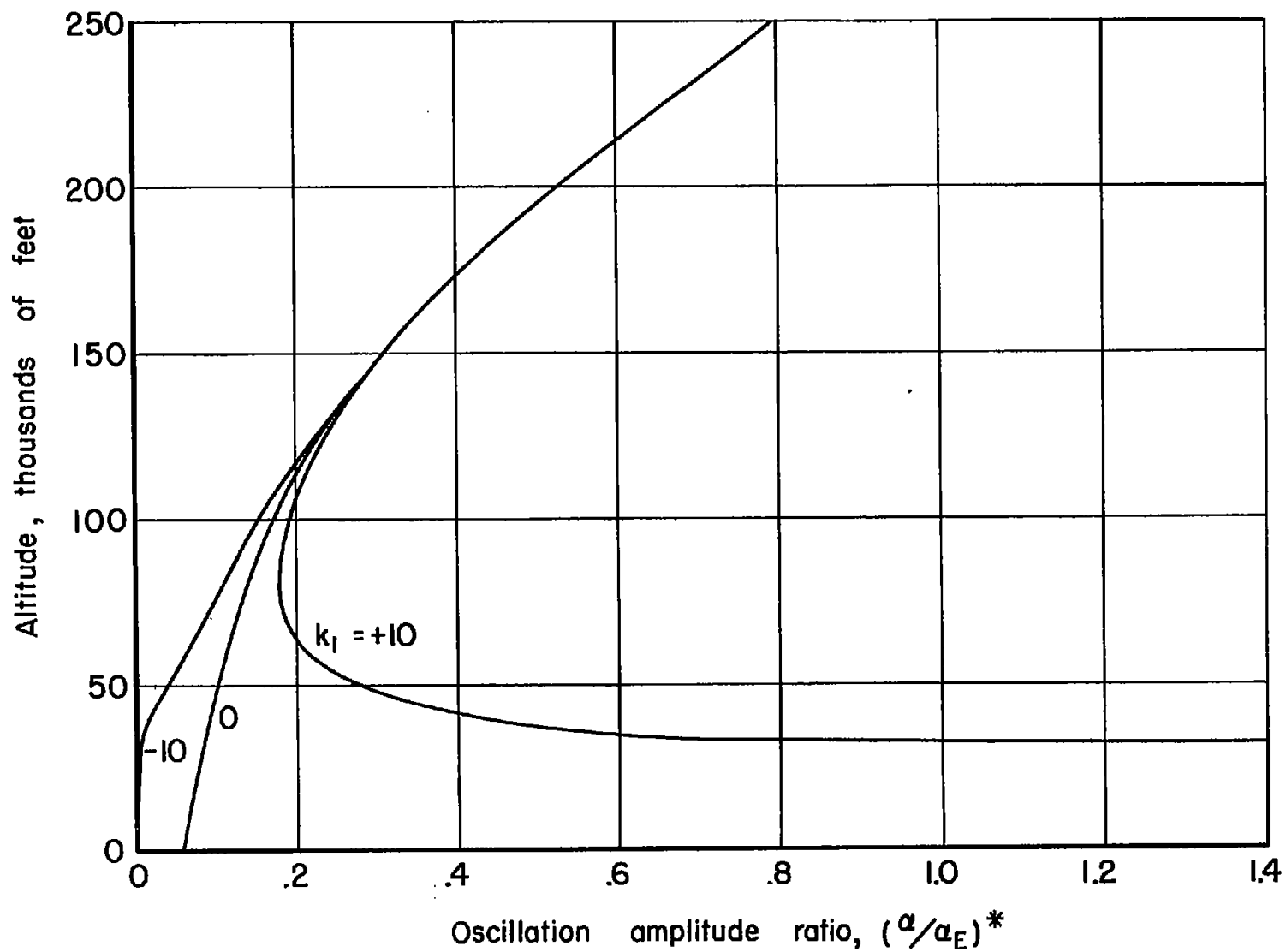
Figure 1.—Effect of parameter k_1 on angular amplitude ratio.
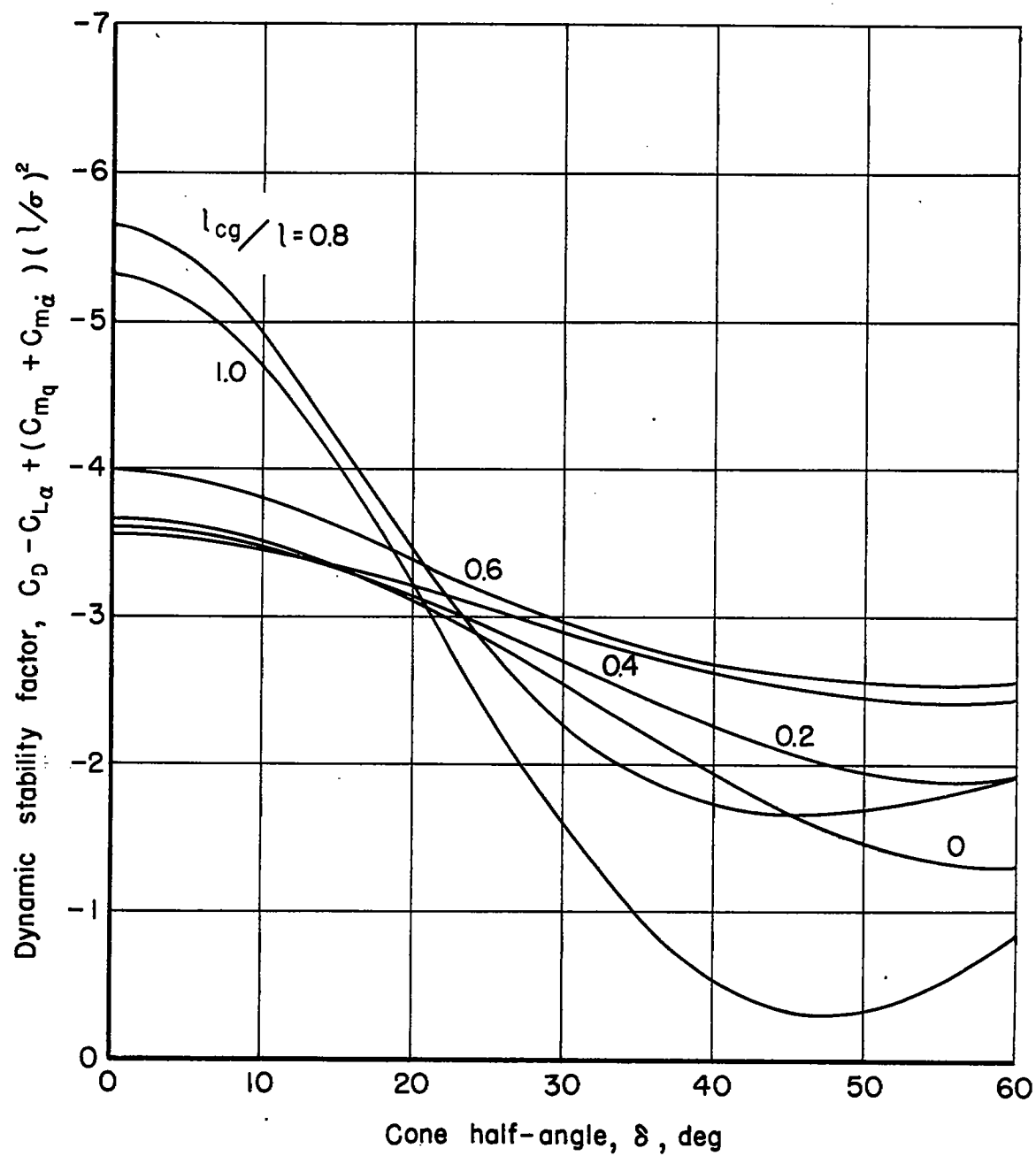
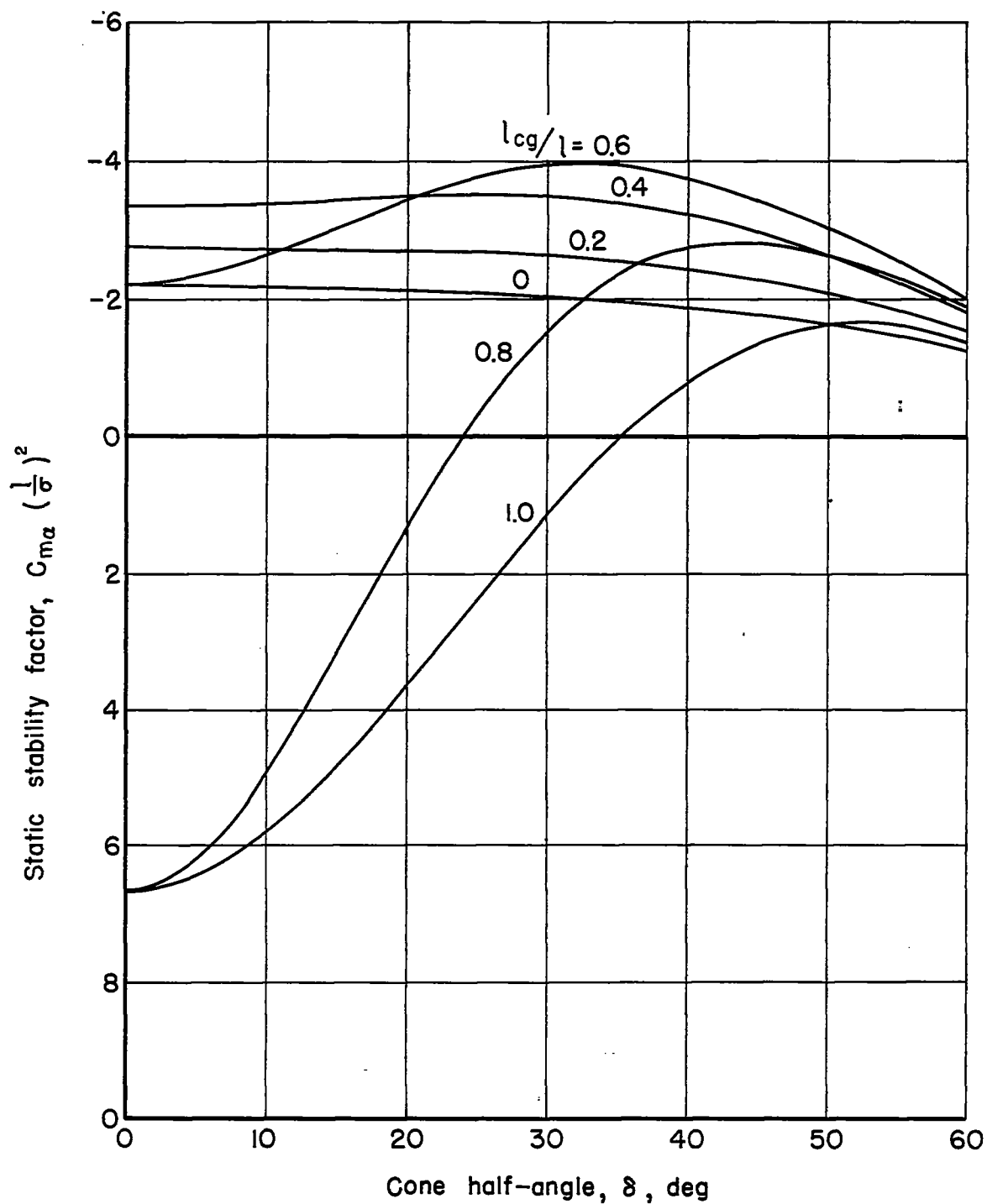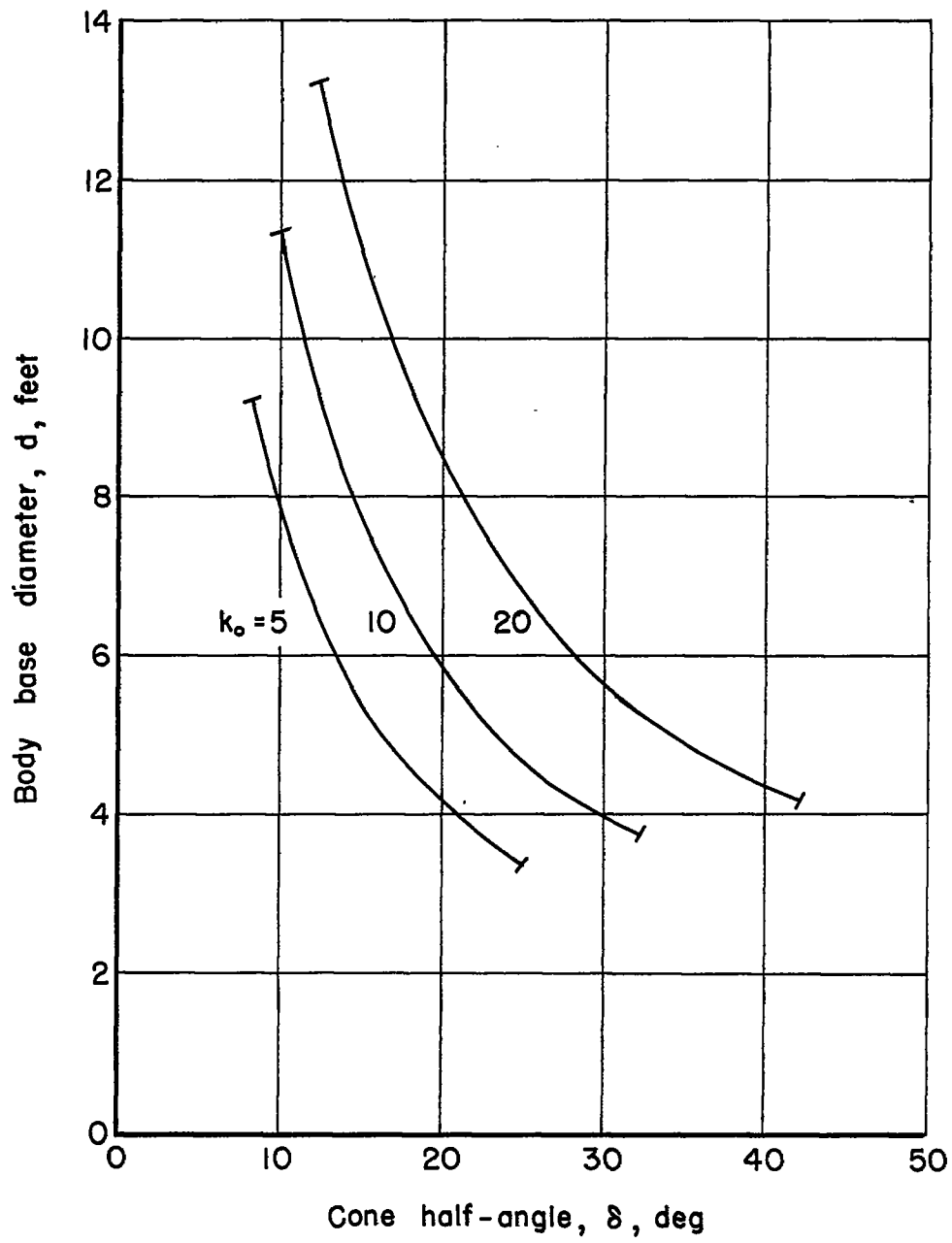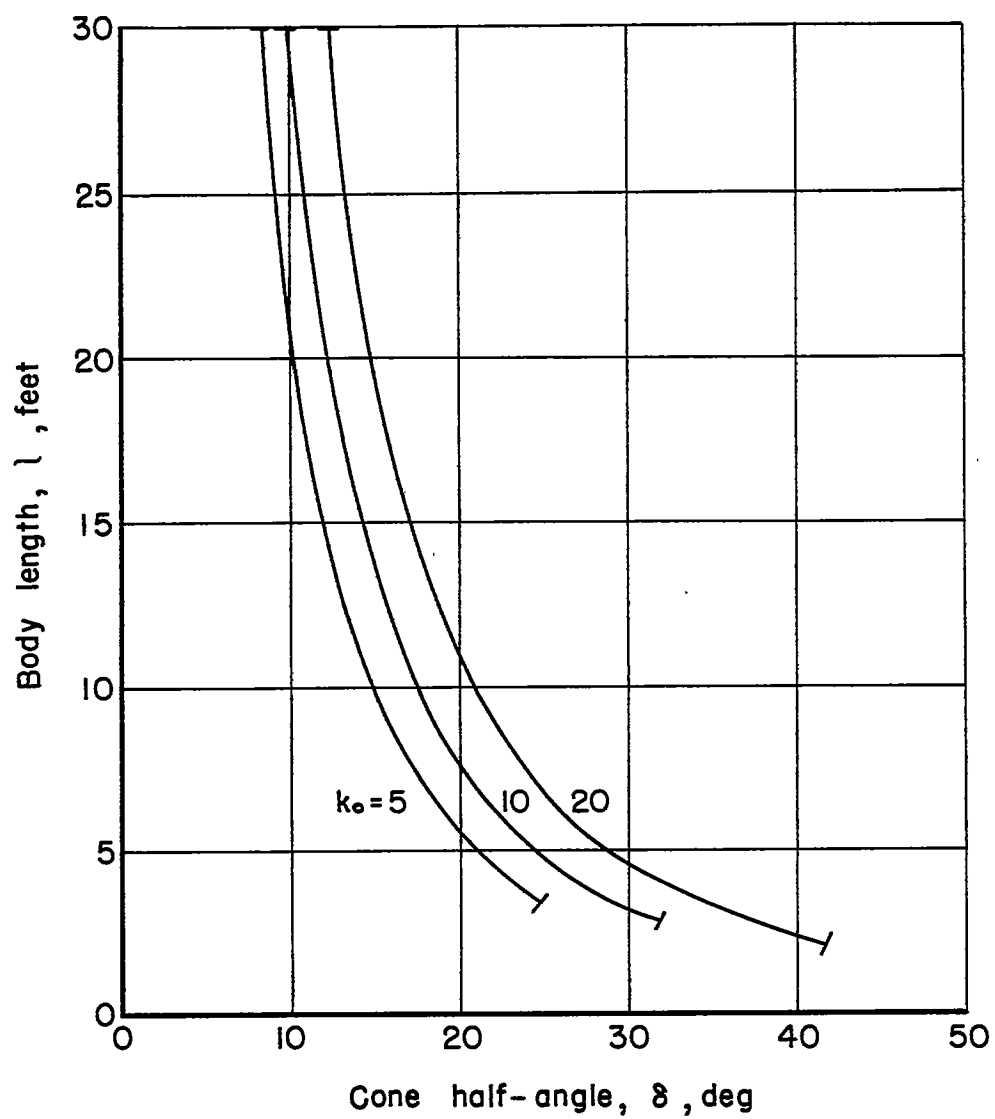Figure 2.— Dynamic stability factors for conical missiles.

Figure 3.– Static stability factors for conical missiles.
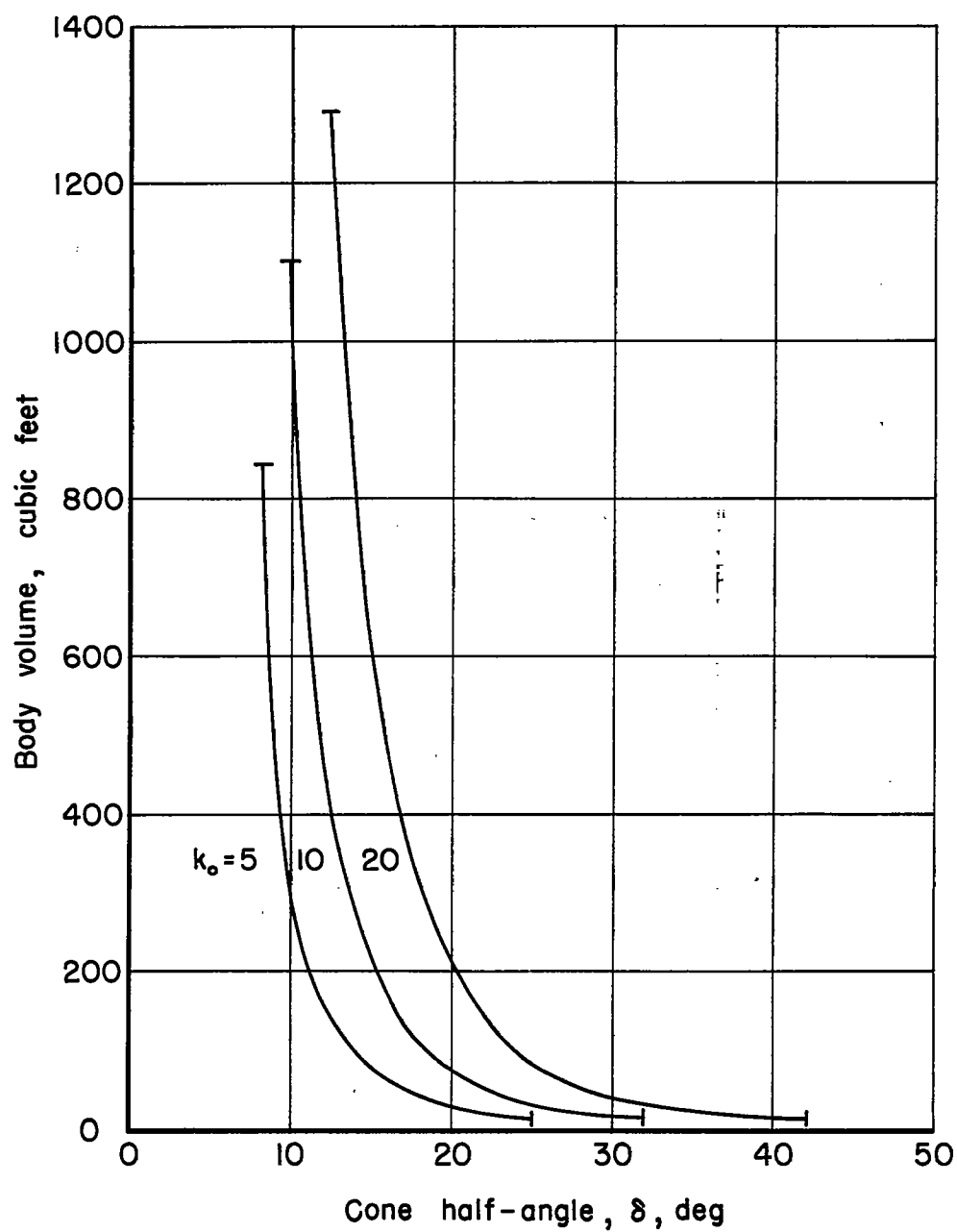
(a) Body base diameter.

Figure 4.- Physical characteristics of example missiles.
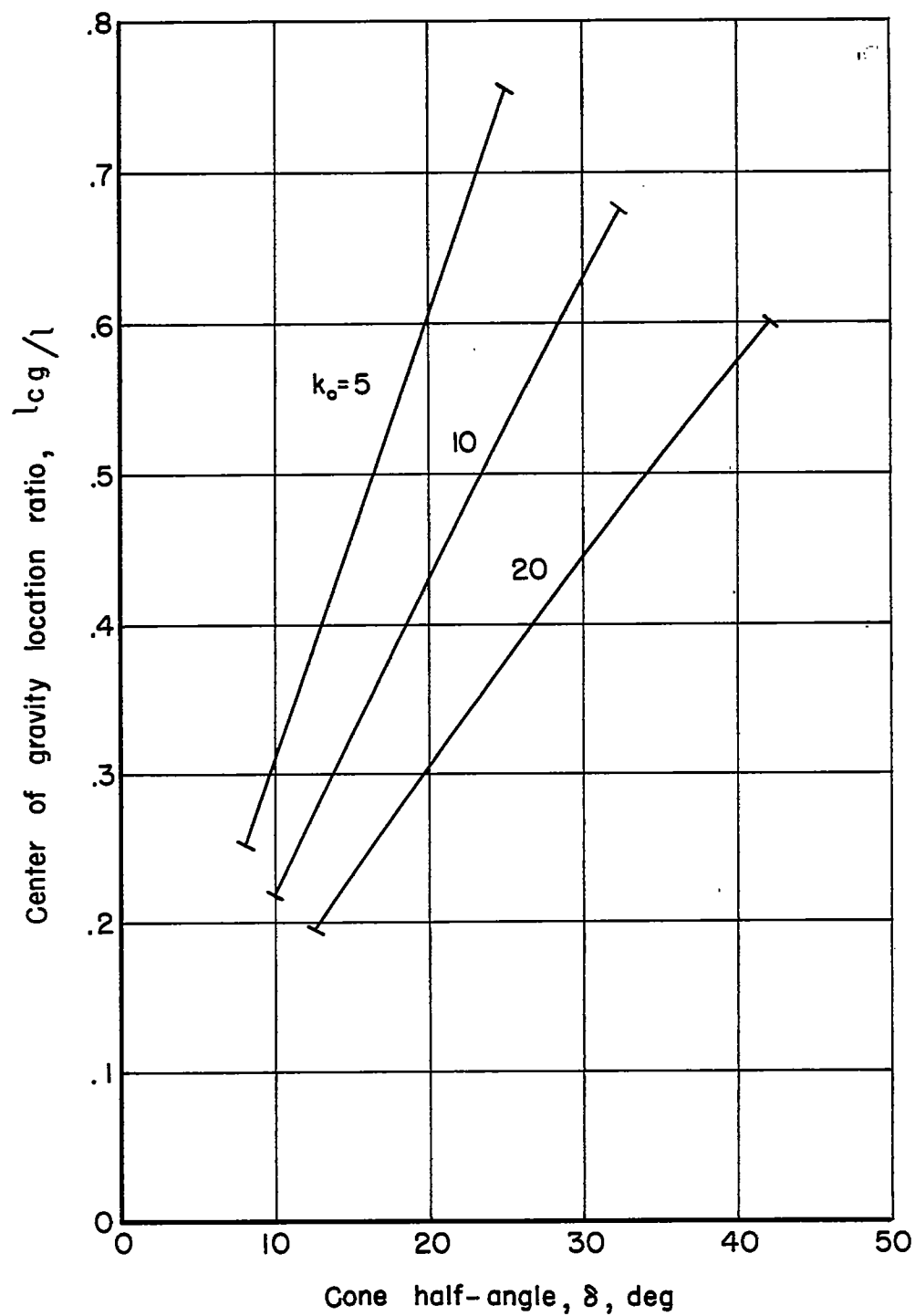
(b) Body length.

Figure 4.- Continued.

(c) Body volume.

Figure 4.- Continued.

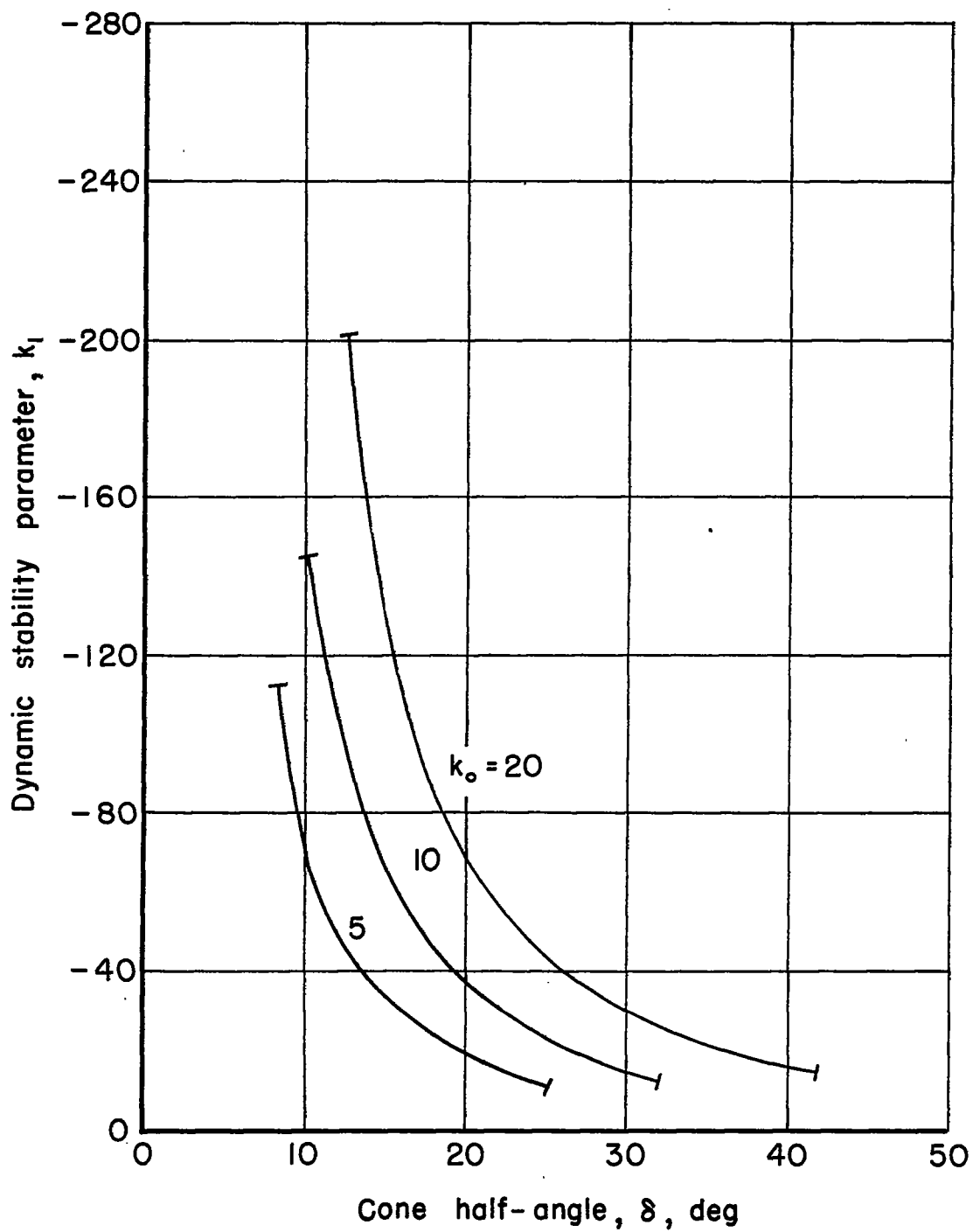(d) Center of gravity position.

Figure 4. – Concluded.

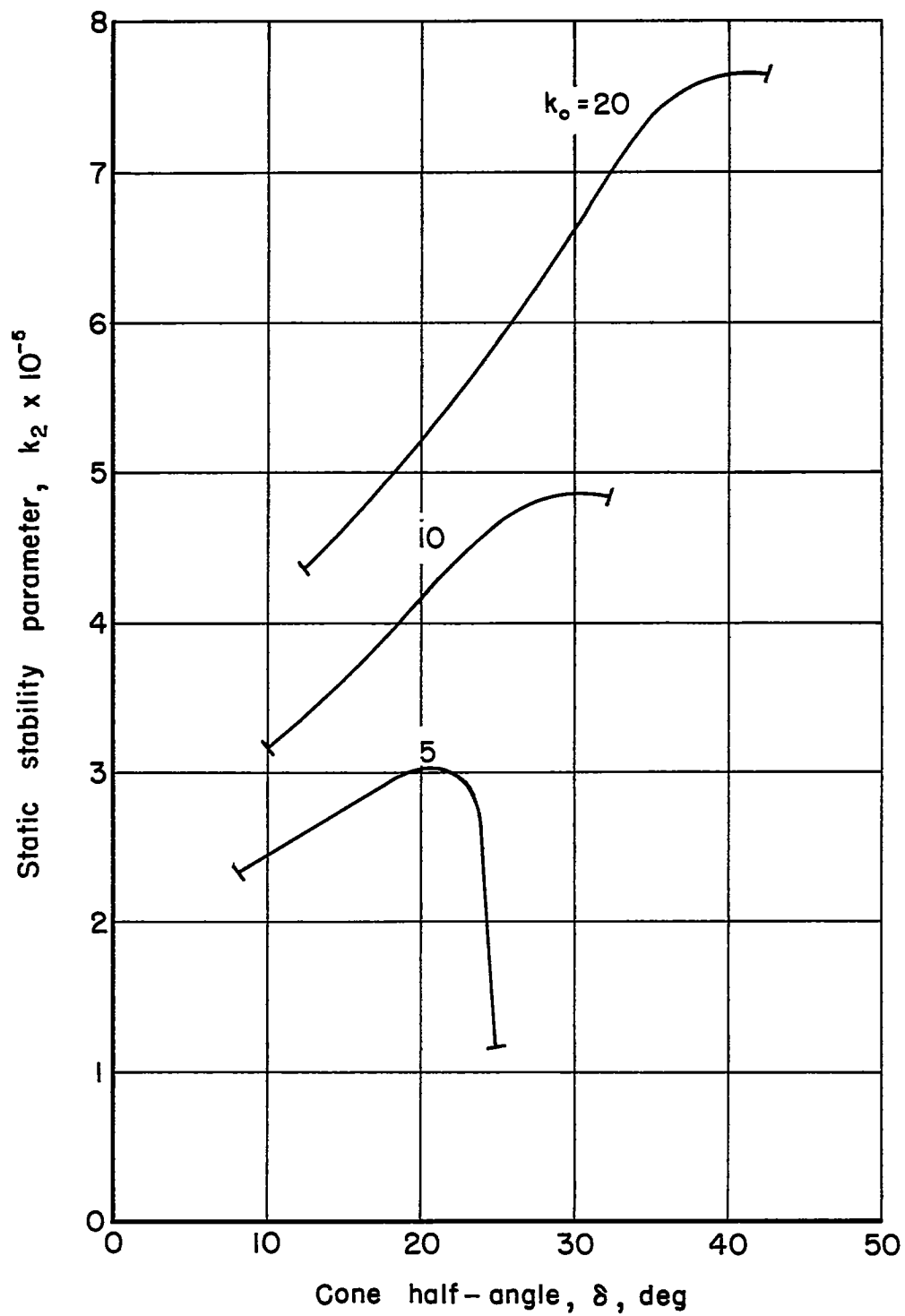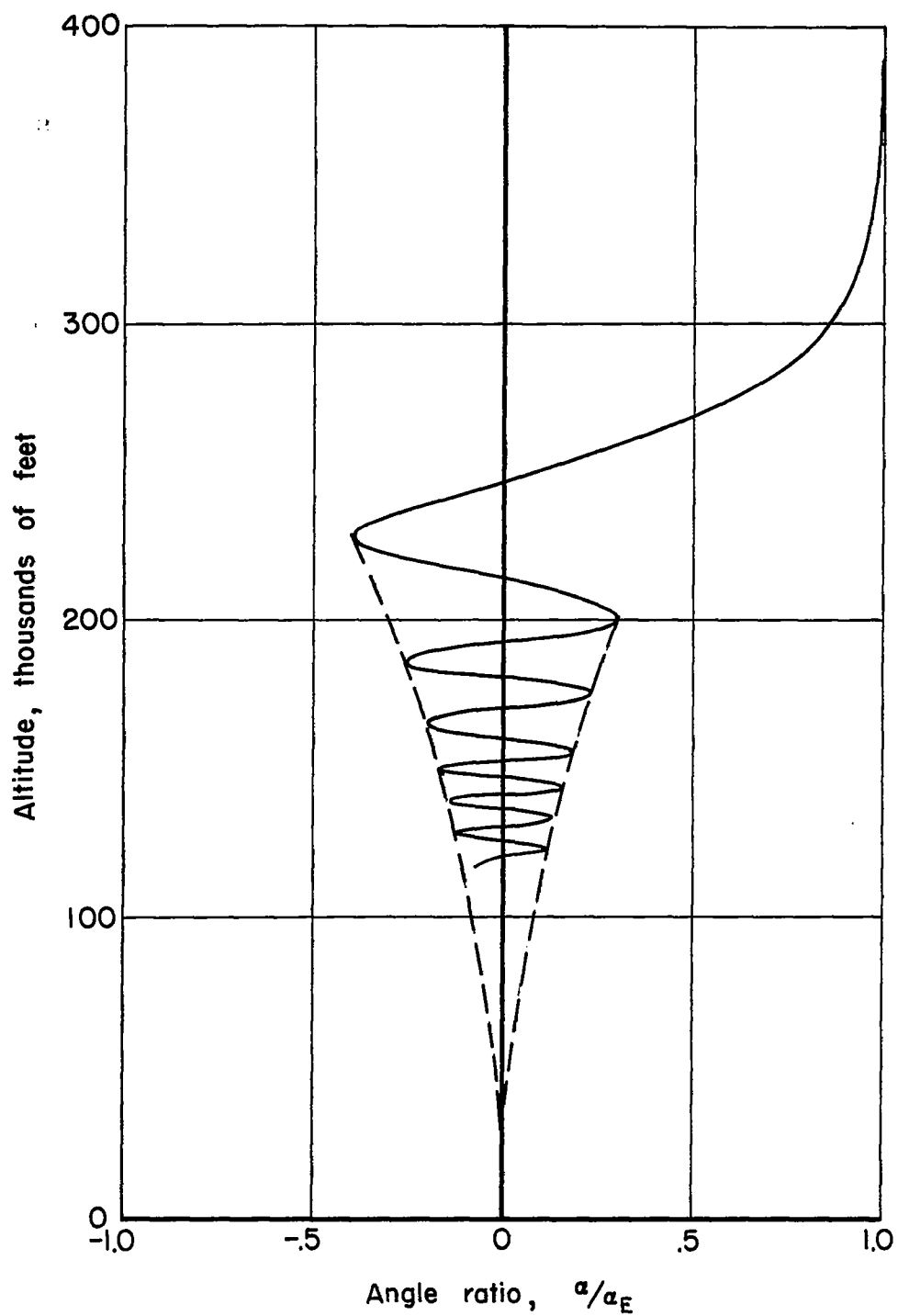Figure 5.- Dynamic stability parameter for example conical missiles.

Figure 6.– Static stability parameter for example conical missiles.

(a) Conical missile of 10 cubic feet with $k_o = 5$

Figure 7.— Altitude variation of oscillations.

Angle ratio, α/α_E
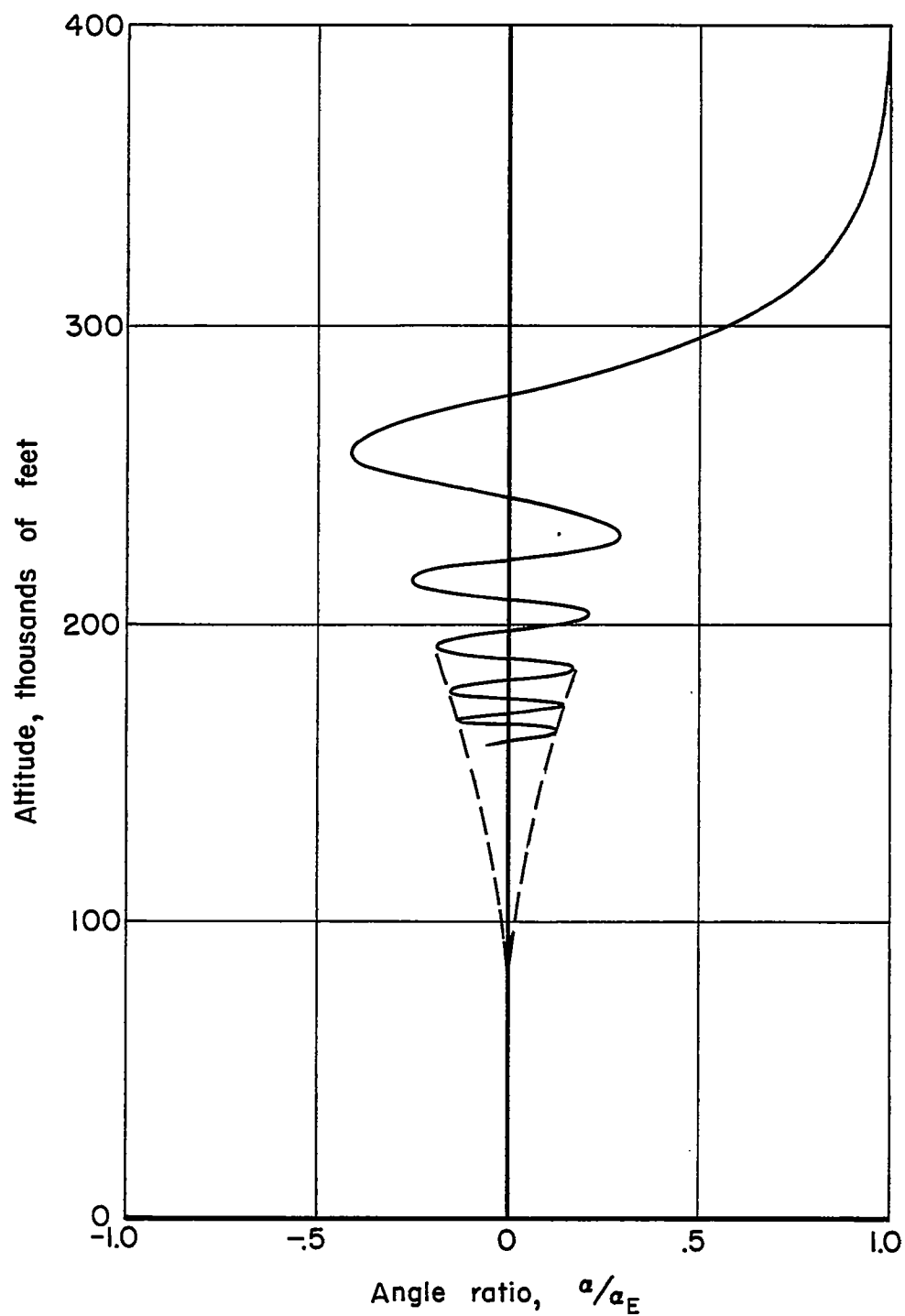
(b) Conical missile of 30 — foot length with $k_o = 20$

Figure 7. — Concluded.
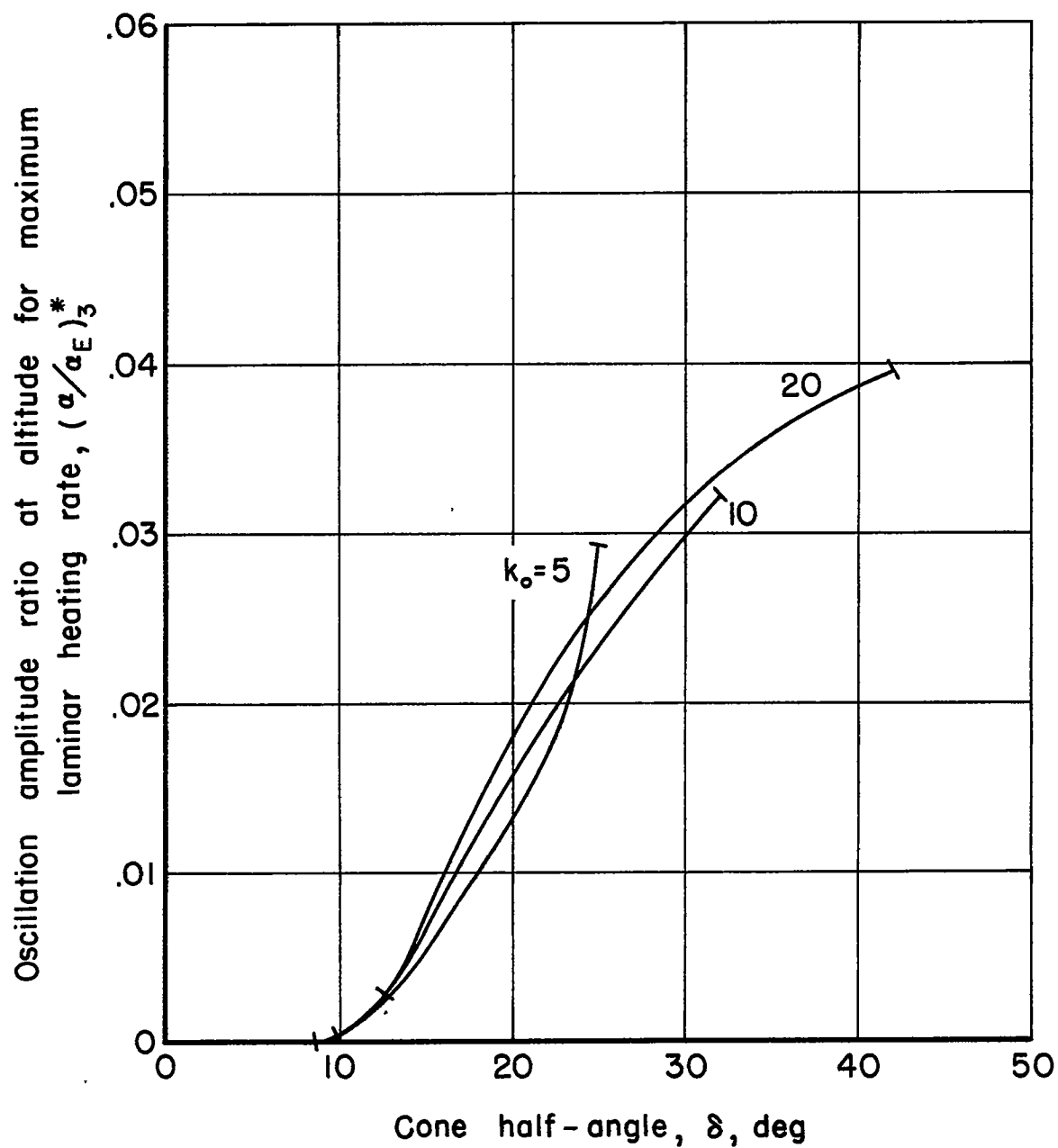
Figure 8.— Amplitude ratio at altitude for maximum laminar heating rate.
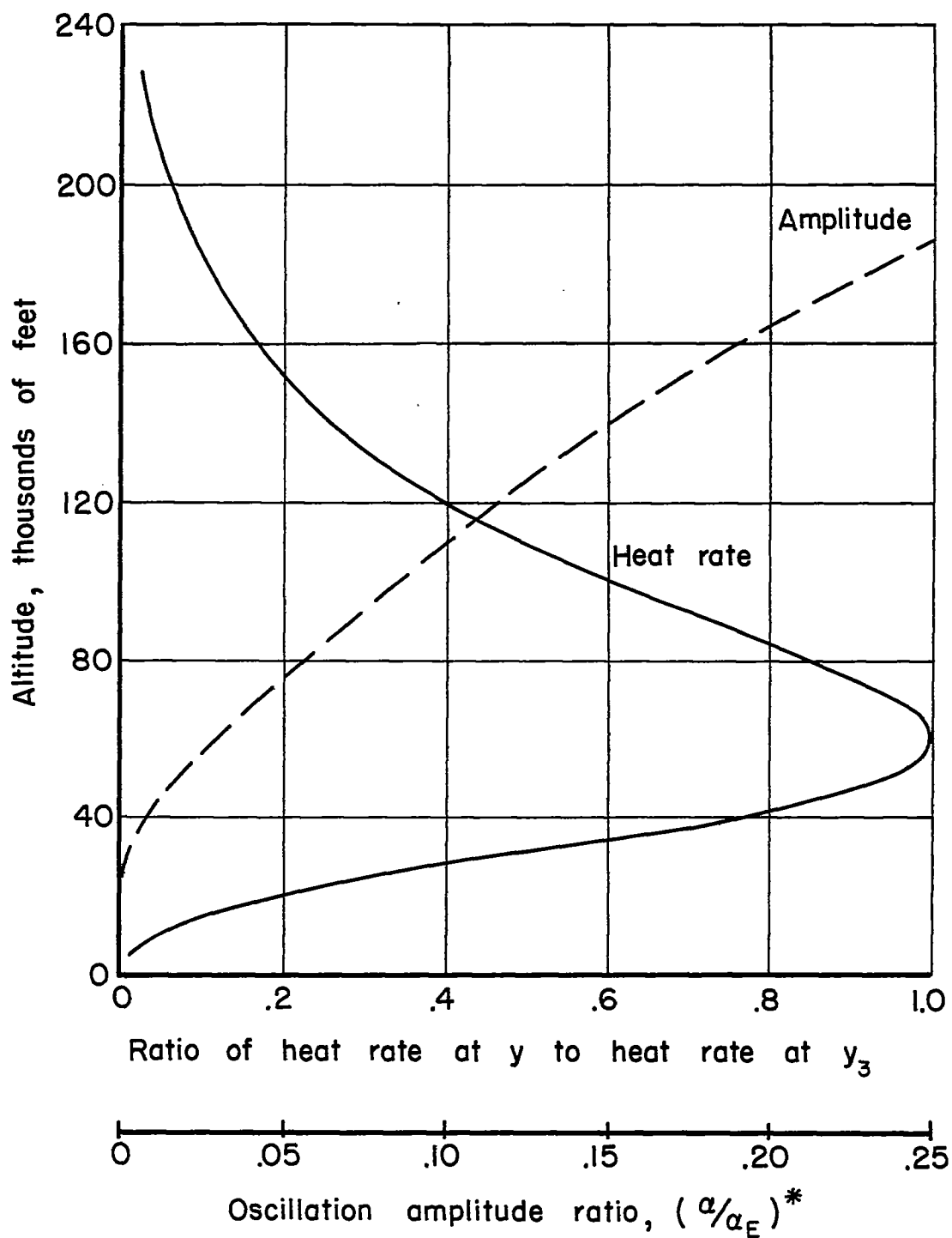
Figure 9.— Laminar heating rate and amplitude ratio as a function of altitude for $k_o = 5$, $\delta = 25°$.
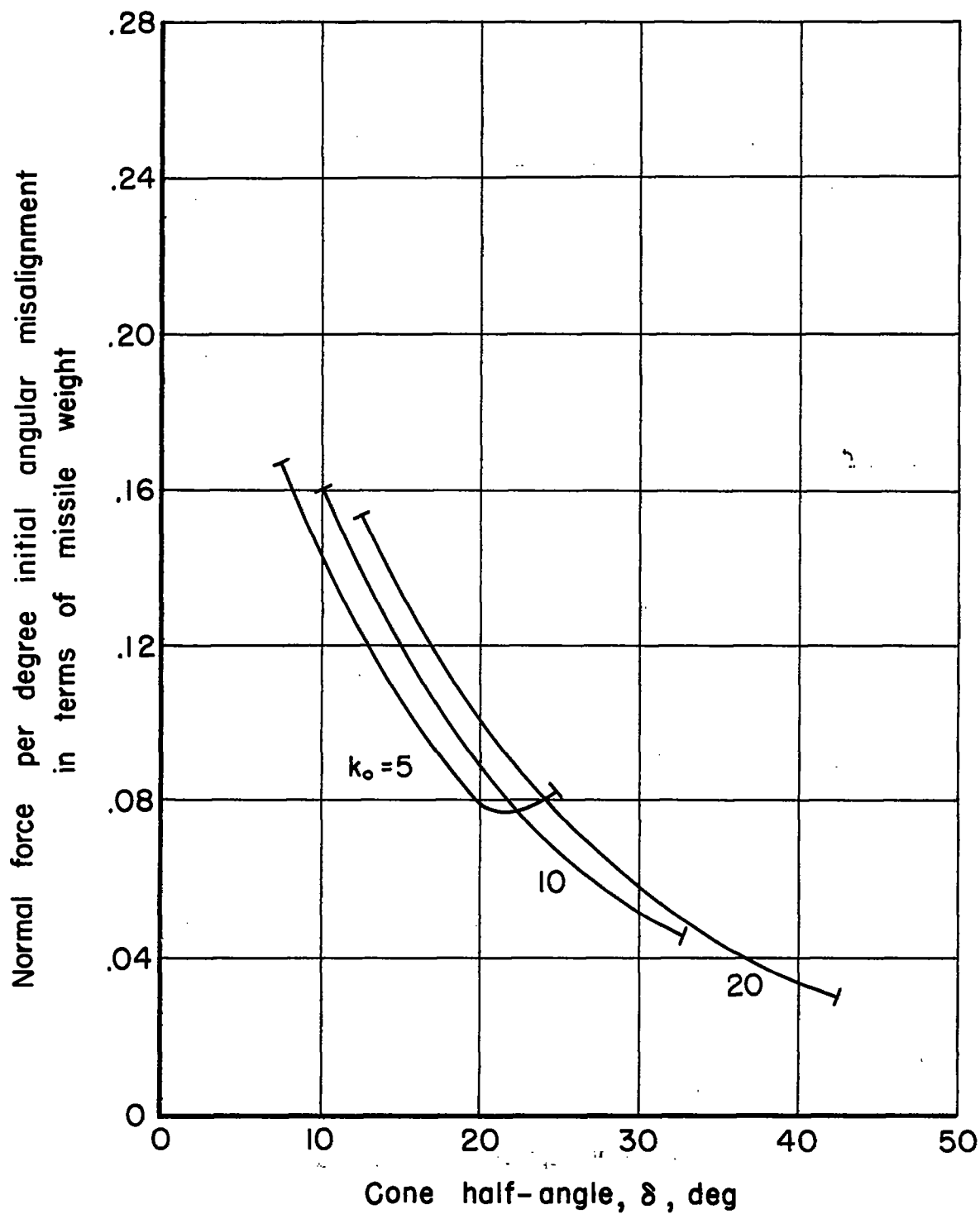
Figure 10.- Maximum normal-force experienced by example missiles.
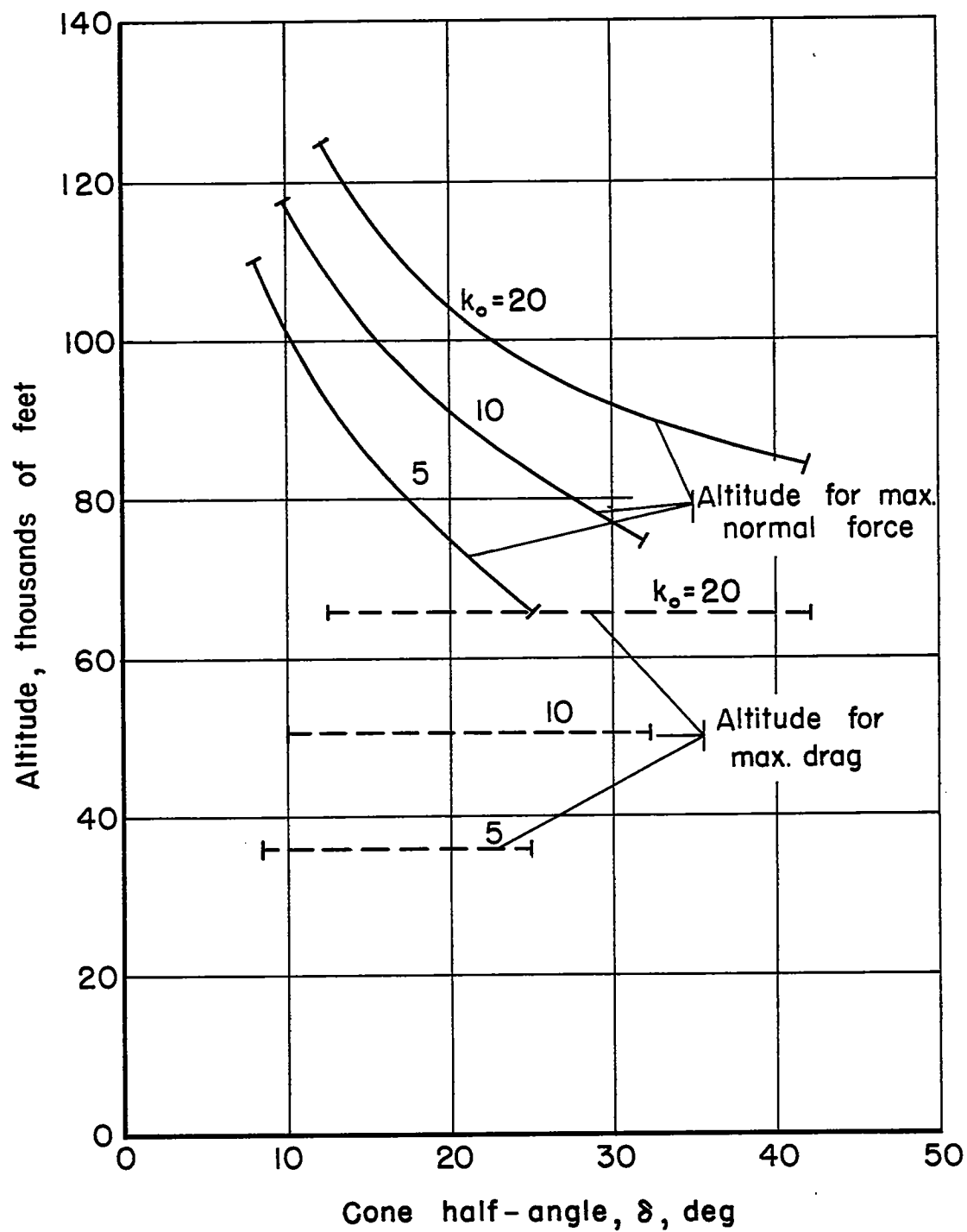
Figure 11.- Altitudes for maximum normal force and drag for example missiles.
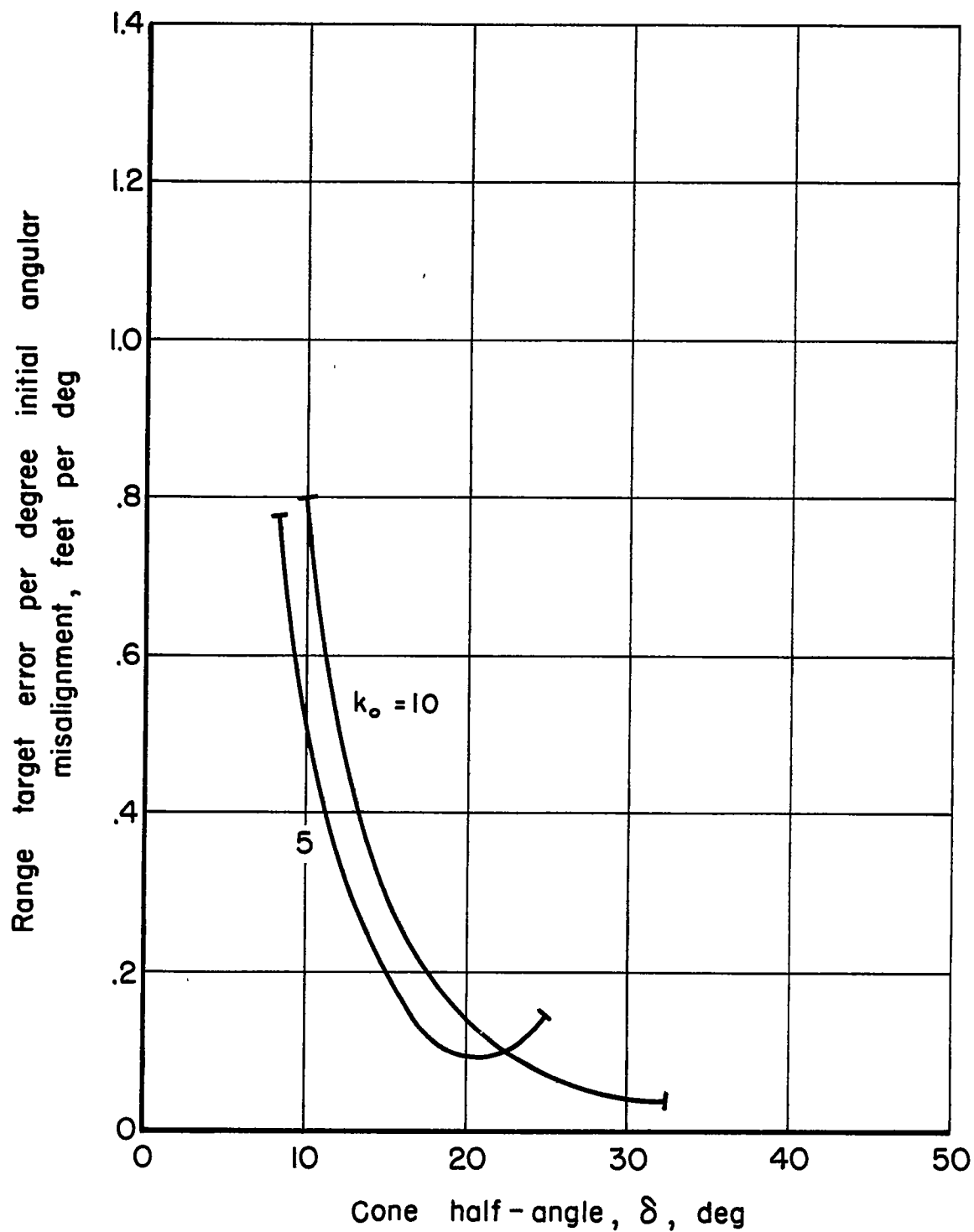
Figure 12. - Range target error per degree initial angular misalignment for example missiles.
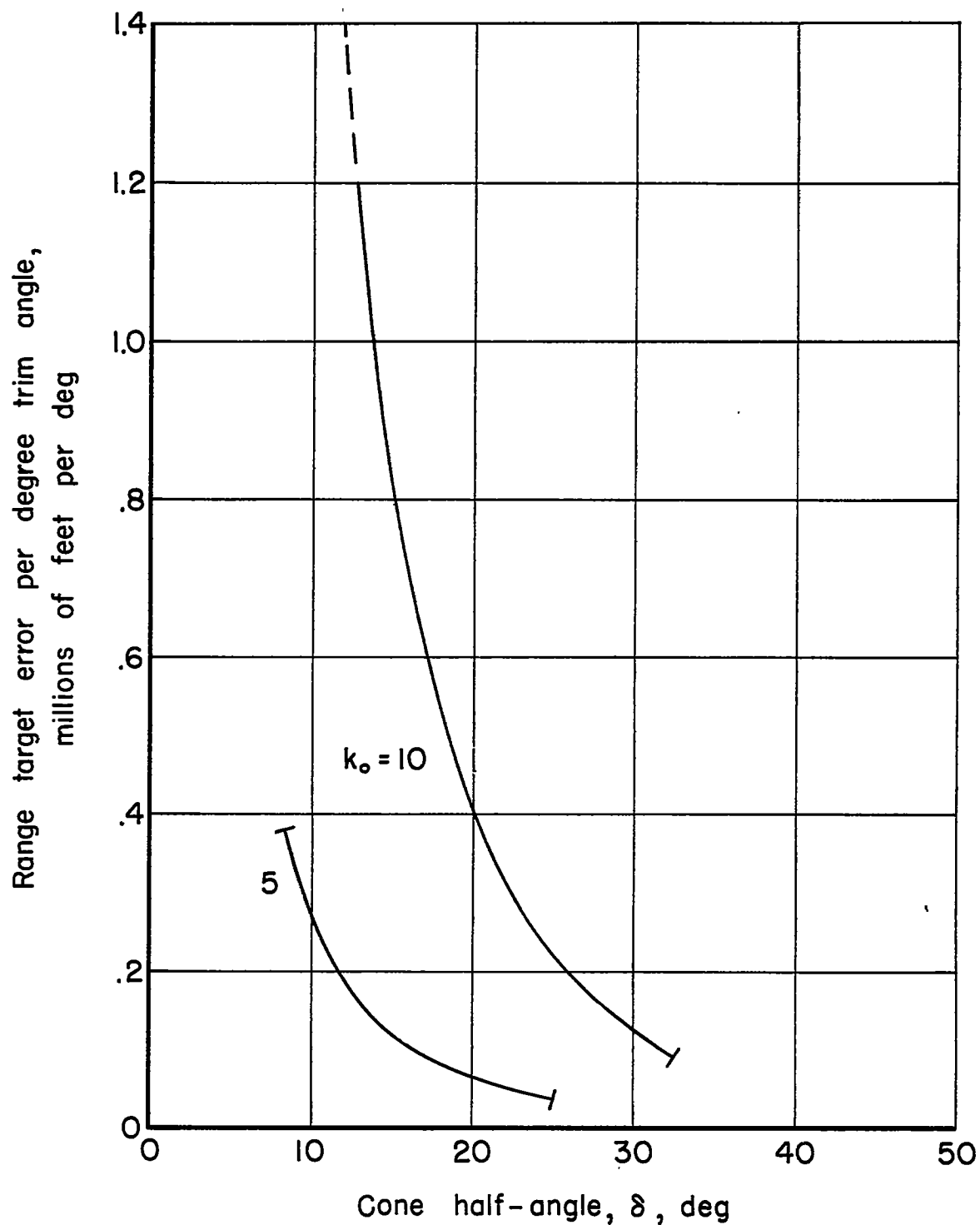
Figure 13.- Range target error per degree trim angle for example missiles.
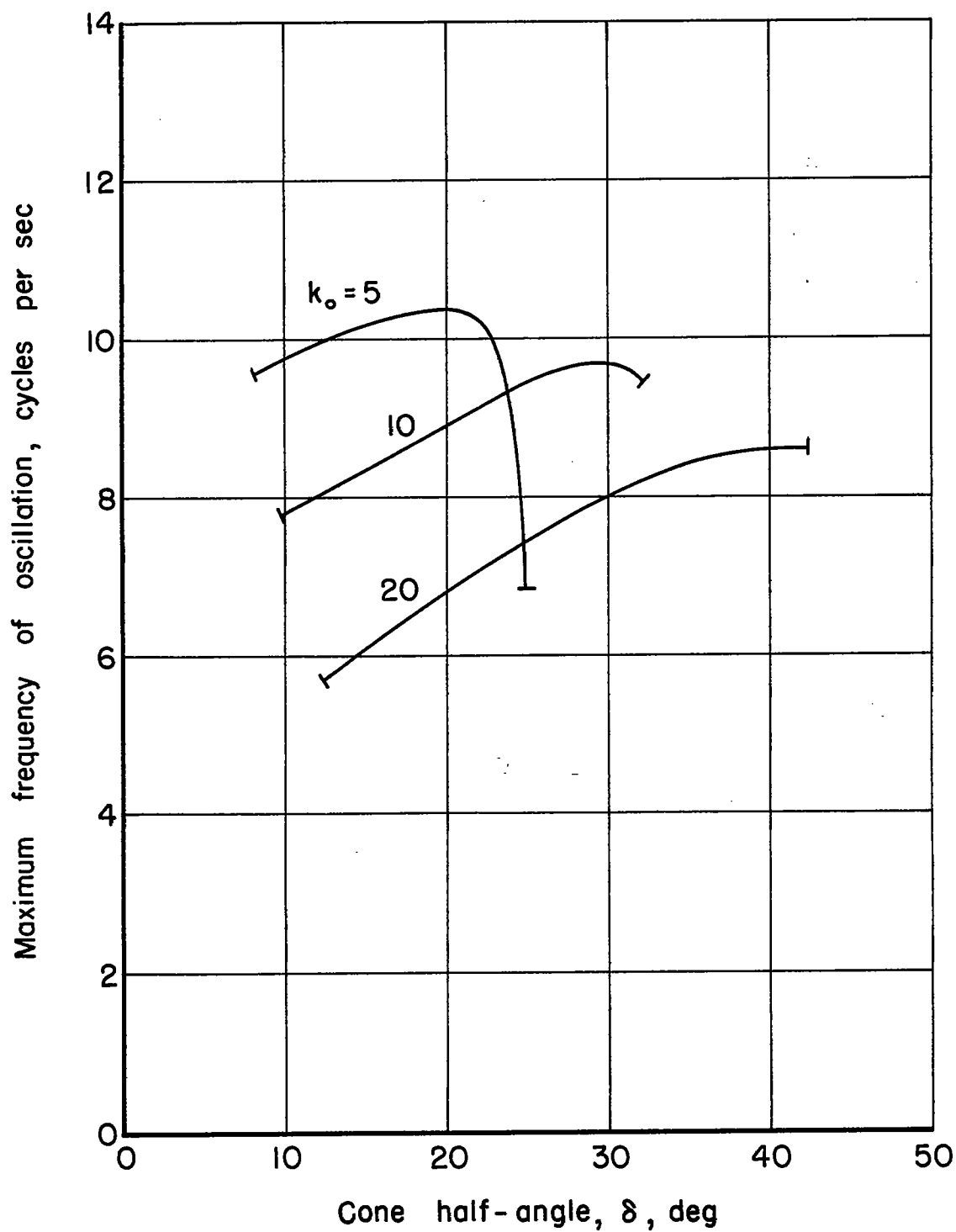
Figure 14.— Maximum oscillation frequencies for example missiles.
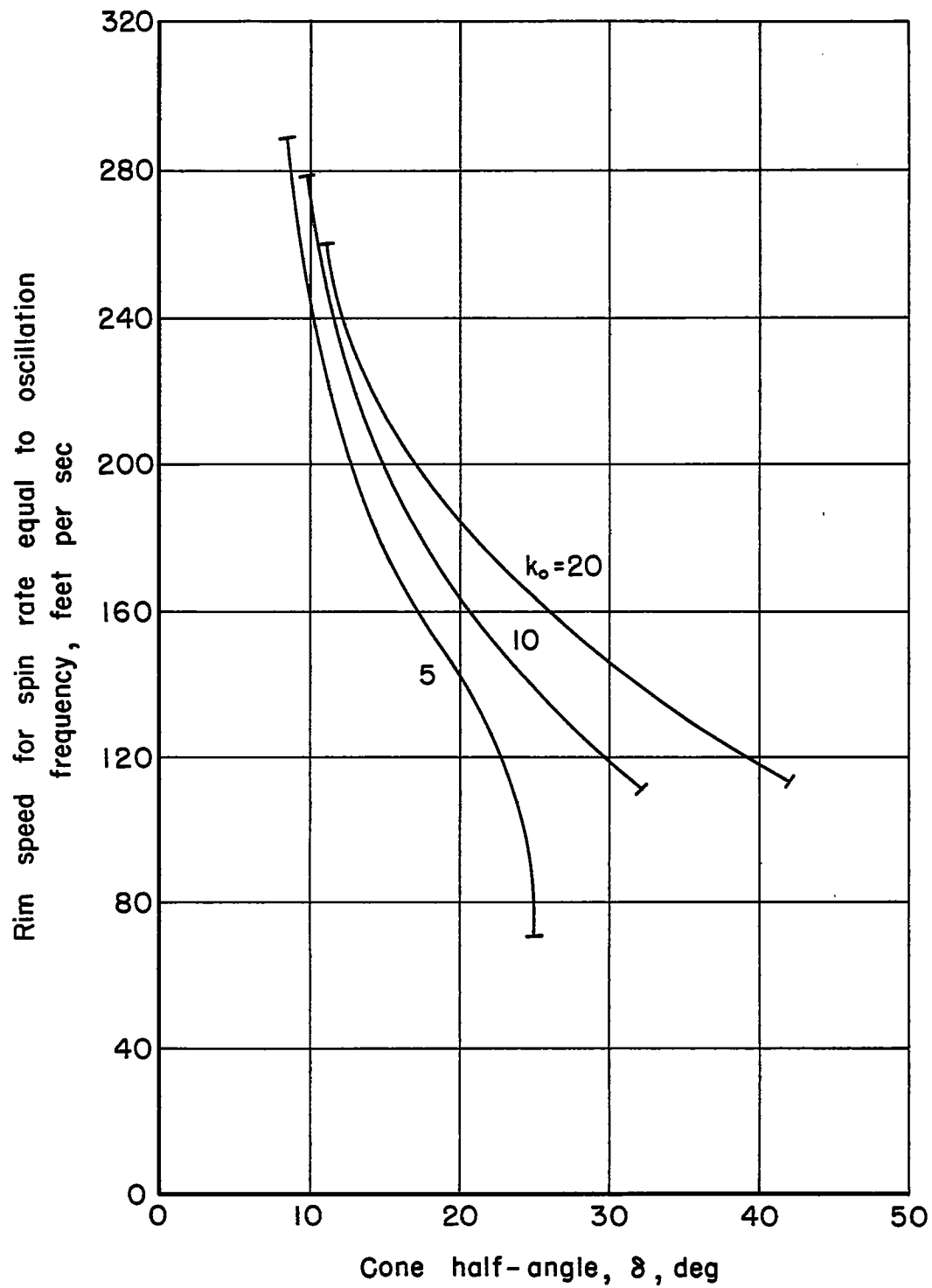
Figure 15.— Rim speed for example missiles if spin rate
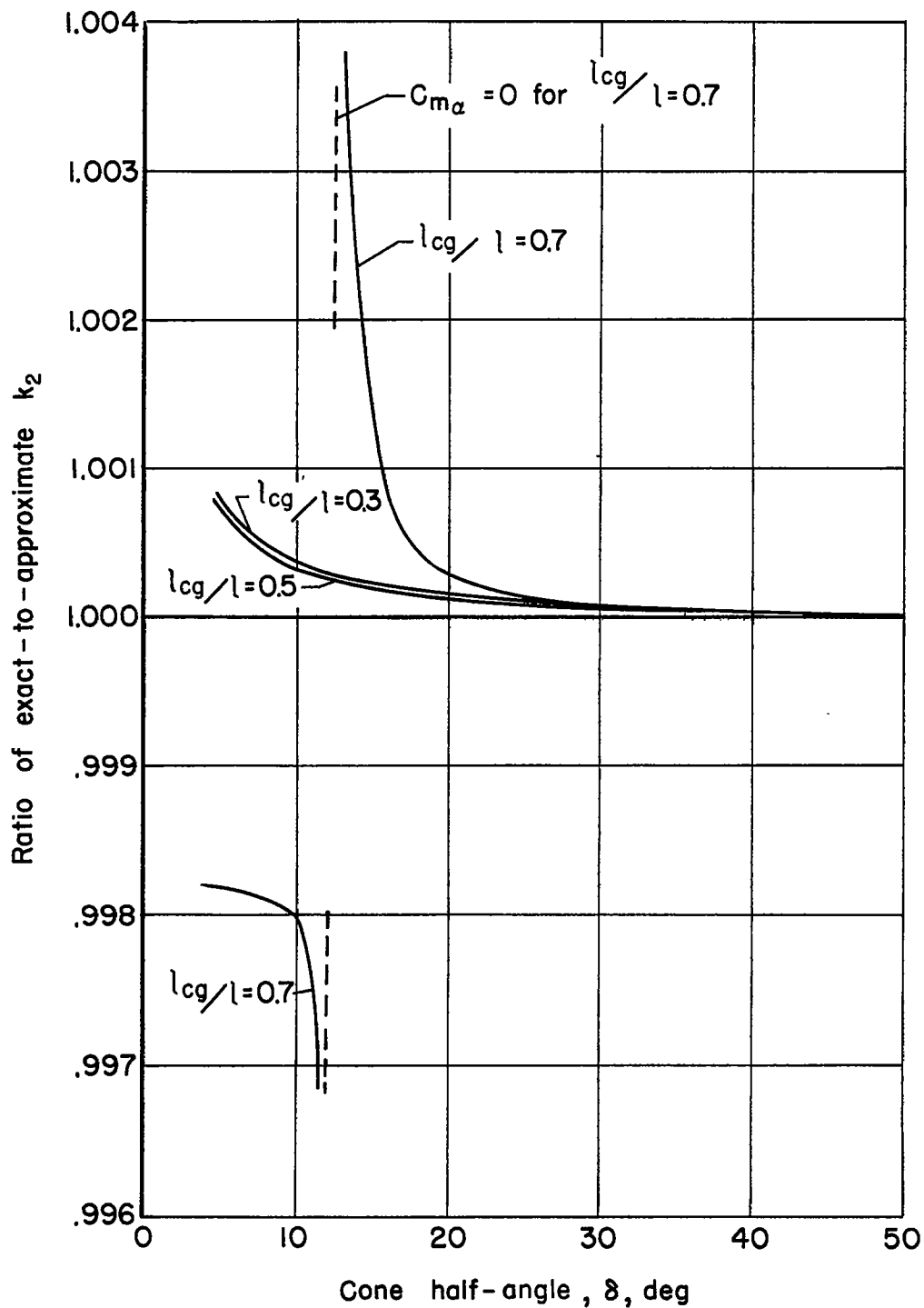equals maximum oscillation frequency.

Figure 16. — Ratio of exact k_2 to approximate k_2 for example of largest probable error as a function of missile-cone half-angle.
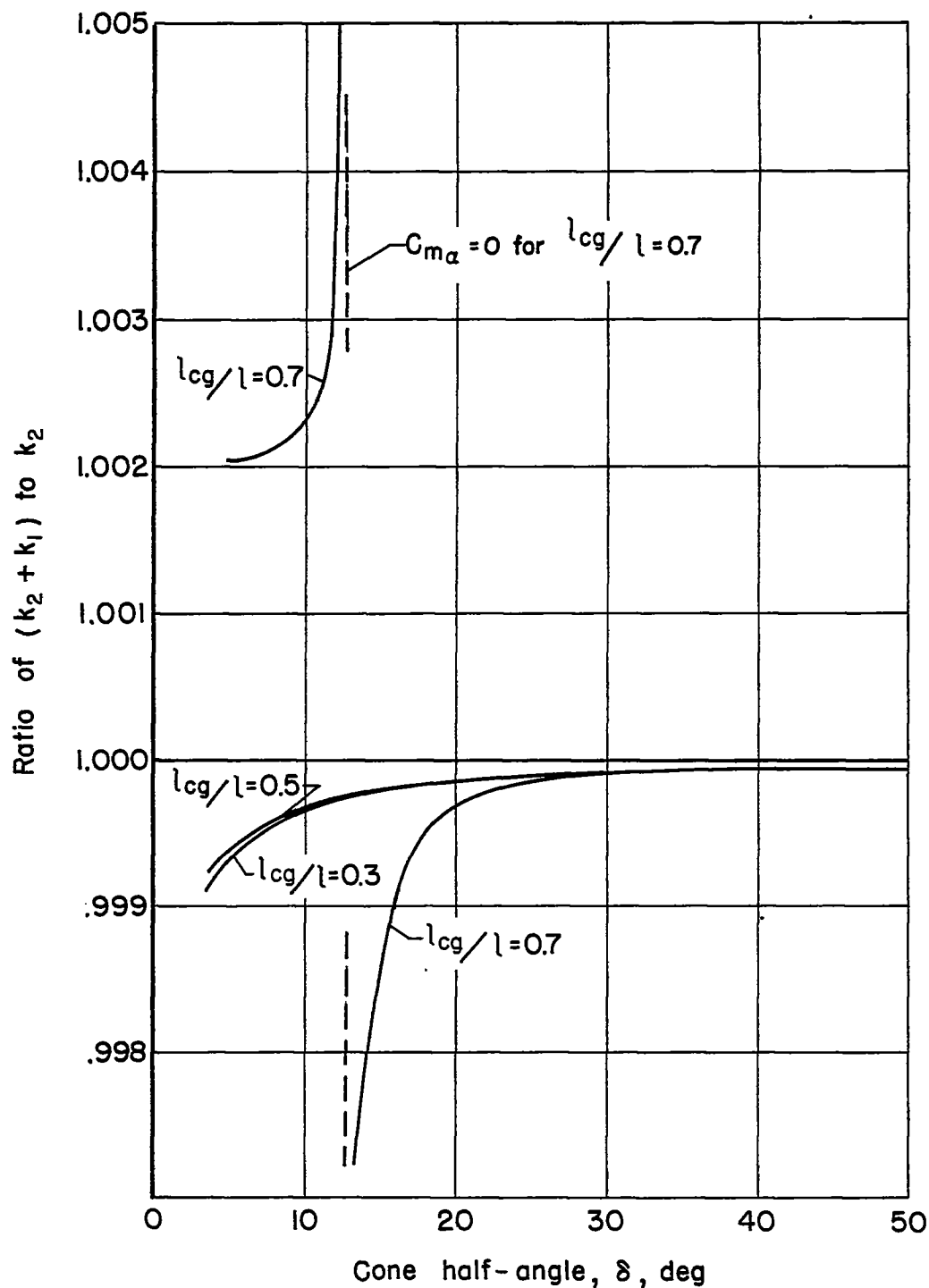
Figure 17. – Ratio of $(k_2 + k_1)$ to k_2 for example of largest probable error as a function of missile-cone half-angle.
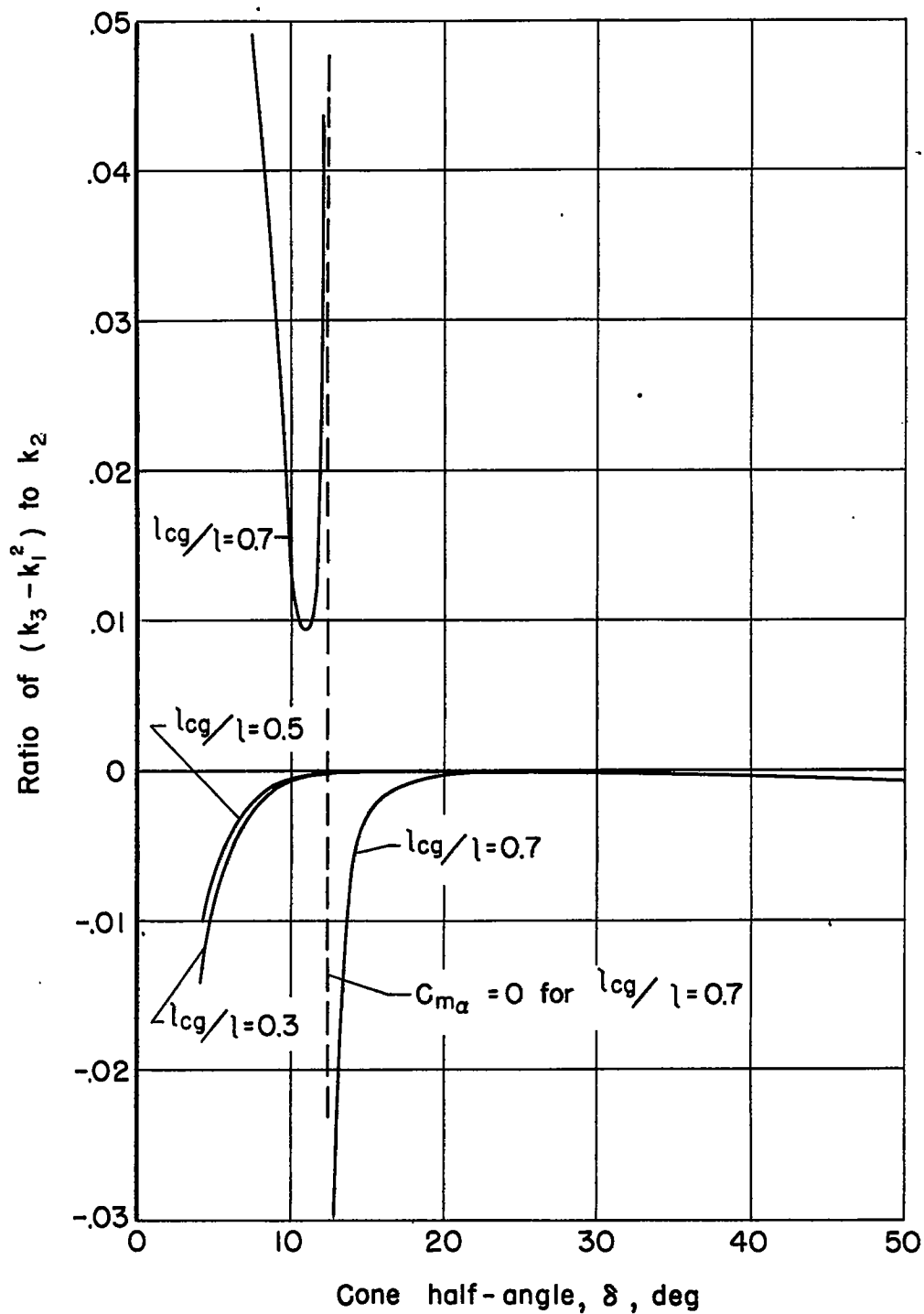
Figure 18. — Ratio of $(k_3 - k_1{}^2)$ to k_2 for example of largest probable importance of $k_3 - k_1{}^2$ as a function of missile-cone half-angle.